

Low energy $\bar{K}N$ interactions and Faddeev calculation of the K^-d scattering length in isospin and particle bases

A. Bahaoui¹, C. Fayard², T. Mizutani³, and B. Saghai^{41, 2, 3, 4}

¹1) *Université Chouaib Doukkali, Faculté des Sciences, El Jadida, Morocco*

²2) *Institut de Physique Nucléaire de Lyon, IN2P3-CNRS, Université Claude Bernard, F-69622 Villeurbanne cedex, France*

³3) *Department of Physics, Virginia Polytechnic Institute and State University, Blacksburg, VA 24061, USA*

⁴4) *Département d'Astrophysique, de Physique des Particules, de Physique Nucléaire et de l'Instrumentation Associée, DSM, CEA/Saclay, 91191 Gif-sur-Yvette, France*

(Dated: July 14, 2003)

$\bar{K}N$ interactions are investigated *via* an effective non-linear chiral meson-baryon Lagrangian. The adjustable parameters are determined by a fitting procedure on the K^-p threshold branching ratios and total cross-section data for $p_K^{lab} \leq 250$ MeV/c. We produce predictions for the $\Sigma\pi$ mass spectrum, and scattering lengths a_{K^-p} , $a_n(K^-n \rightarrow K^-n)$, $a_n^0(\bar{K}^0n \rightarrow \bar{K}^0n)$, and $a_{ex}(K^-p \rightarrow \bar{K}^0n)$. The $\bar{K}N$ amplitudes thus obtained, as well as those for other two-body channels (πN , NN , and YN) are used as input to predict the scattering length A_{K^-d} , for which we have devised a relativistic version of the three-body Faddeev equations. Results for all two- and three-body coupled channels are reported both in isospin and particle bases. All available $\bar{K}N$ data are well reproduced and our best results for the K^-p and K^-d scattering lengths are $a_{K^-p} = (-0.90 + i0.87)$ fm, and $A_{K^-d} = (-1.80 + i1.55)$ fm, respectively.

PACS numbers: PACS numbers: 11.80.-m, 11.80.Jy, 13.75.-n, 13.75.Jz

I. INTRODUCTION

The present paper is devoted to the study of the K^- -deuteron scattering length A_{K^-d} by exploiting a relativistic version of the three-body Faddeev equations in which the principal two-body input is based on an effective non-linear chiral meson-baryon Lagrangian in the strangeness $S = -1$ sector. A preliminary version has been reported in Ref.[1]. Below we shall begin with a survey on the two-body $\bar{K}N$ amplitudes which are the central input to our present enterprise, as well as the evolution of the low energy K^-d physics. In this way we hope that our motivation be clear to the reader.

While the low to medium energy *kaon-nucleon* processes (say, $p_K^{lab} \leq 1.5$ GeV/c) have been known to show no significant structure up to the pion production threshold in the KN channel, its u -channel counterpart: the $\bar{K}N$ channel, presents quite a rich structure (resonances, possible bound states in the continuum, etc.): see for example [2, 3]. For the most recent discussions on both experimental and theoretical fronts, see, for example, Olin and Park [4]. The thus mentioned characteristics may be understood within a simple quark model where the quark structure of \bar{K} , \bar{K} and N are known to be $q\bar{s}$, $\bar{q}s$, and qqq , respectively with q being u and/or d quarks. In this picture the $\bar{K}N$ system may be rearranged to become a combination like $(\bar{q}q)(sqq)$ which may be identified, for example, as πY , ($Y = \Lambda, \Sigma$) in terms of the lowest-lying octet hadrons, or to generate strangeness $S = -1$ hyperon resonances. On the contrary, such a scenario does not materialize for the KN system in which the antiquark involved is \bar{s} , hence the corresponding low energy process is uniquely the elastic scattering of K and N . So both theoretically and experimentally, the $\bar{K}N$ ($S = -1$) system has been drawing much more attention than the KN ($S = 1$) channel.

Of particular interest in this regard has been the K^-p channel near threshold. It is dominated by the below-threshold resonance $\Lambda(1405)$ to which it strongly couples. This resonance decays almost exclusively to $\pi\Sigma$. One of the intriguing subjects related to this resonance has been on its dynamical origin: whether it is a hadronic bound state of K^-p embedded in continuum (since it is located above the $\pi\Sigma$ threshold), or a three-quark baryon resonance (or something more exotic). Whereas no definite conclusion has been drawn based on the scattering data analyses by forward dispersion relation [2, 3], a recent effective chiral Lagrangian approach [5] has presented a convincing picture in favour of the K^-p ($I = 0$) bound state, as we shall discuss later in the context of the objective of the present paper. A more down to the earth, but quite important problem has been the K^-p scattering length a_{K^-p} , that dictates the threshold characteristics of the K^-p interaction. For this quantity the so-called *kaonic hydrogen puzzle*, see e.g. Ref. [6], had disturbed the community engaged in low energy meson-baryon interactions for quite a long time. Briefly, the puzzle originated from the fact that the real part of a_{K^-p} extracted from the $1s$ atomic level shift (due to the strong interaction) of the kaonic hydrogen [7] had an opposite sign to the one obtained from the analyses of the K^-p scattering amplitude.

Despite the persistence of this puzzle, several pioneering works on the low energy negative kaon-deuteron (K^-d) scattering by solving three-body equations were performed by simply disregarding the information from the kaonic hydrogen. The first study of that type on the K^-d elastic scattering at low energies was performed as early as 1965 [8] by adopting simple S -wave rank one (non-local) separable interactions for the $I = 0, 1$ $\bar{K}N$ channels and for the 3S_1 deuteron channel as basic two-body ingredients. For the $\bar{K}N$ interaction the potentials were fitted to reproduce the complex-valued K^-p scattering length known from the amplitude analysis at that time (see for example [9]). The principal objective of the work was to see the convergence properties of the multiple scattering series: at low energies they found that the single and double scattering contributions were far from sufficient. An extension of this work to the three-body break up channels: $K^-d \rightarrow K^-np, \bar{K}^0 nn$ was performed by the same authors by deforming the momentum integration in the complex plane to avoid the anomalous threshold branch cuts due to the final state NN interactions [10]. The result turned out to be insufficient for discriminating the different K^-p input amplitudes by comparing with the data, as the two-body input were incomplete, along with insufficient statistics for the data. However, the methods developed served in motivating later attempts for studying the three-body final states from the theoretical side. Also the same authors improved their first elastic scattering calculation in Ref. [8] by incorporating the isospin breaking effect manifested in the mass difference between \bar{K}^0 and K^- as well as between n and p , which resulted up to an about 10% difference in the cross section [11]. Later Myhrer [12] studied the role of the $\Lambda(1405)$ resonance in the threshold K^-d scattering by assuming a simple resonance form for the input K^-p amplitude. Here again the insufficiency of few first iterations of the multiple scattering series was found in the presence of a two-body resonance. This was then followed by using improved $\bar{K}N$ amplitudes that took into account the effect of coupling to the physically accessible πY , ($Y = \Lambda, \Sigma$) channels and, though implicitly, the effect of $\Lambda(1405)$ [13]. In this regard one should be reminded that in the earliest works mentioned above [8, 11] those effects were implicitly represented only by the complex-valued $\bar{K}N$ scattering lengths. To summarize, all the models mentioned here summed up multiple scattering series driven by an S -wave $\bar{K}N$ scattering with a spectator N and a 3S_1 NN scattering in the presence of a \bar{K} spectator. We will refer to this type of models as *Single-Channel Approach*.

The next generation of theoretical endeavour [14–17] may be characterized by explicitly taking into account the three-body channels involving hyperons: πNY , ($Y = \Lambda, \Sigma$), where Y is produced from the $\bar{K}N \rightarrow \pi Y$ reactions in the presence of a spectator nucleon. Also included were the two-body interactions πN with a spectator Y as well as YN with π as a spectator. In this way genuine three-body unitarity was guaranteed to hold. Common to all three works cited here is the way to construct all the two-body input amplitudes to the three-body equations. Apart from the NN deuteron channel, all the two-body amplitudes: coupled $\bar{K}N$ - πY channels, πN , as well as coupled NY - NY channels, were assumed to be obtained from rank one separable potentials (mostly in S -waves) where the strengths and ranges were adjusted to fit the available cross sections, etc. Isospin was assumed to be conserved exactly so that the number of channels to deal with in the two-body input as well as in the three-body equations be contained as manageable. This will be termed as the *Multi-Channel Approach* as compared with the single-channel one mentioned earlier.

The first two of those multi-channel approaches [14, 15] were dedicated to the near threshold break-up reactions: $K^-d \rightarrow \pi NY$, where data exist for the reaction rates, the final mass spectra $m(p\Lambda)$, the neutron momentum spectra in the final $n\Sigma^-\pi^+$ as well as in $n\Sigma^+\pi^-$ three-body channels [18, 19]. The models were able to reproduce the experimental trends depending upon which combinations of signs in the non-diagonal amplitudes such as $\bar{K}N \rightarrow \pi\Sigma$, $\Lambda N \rightarrow \Sigma N$ should be adopted. Note that those amplitudes determined by fit to the corresponding cross sections are unique up to an overall sign, or phase in more general terms, unless additional constraints from, say, some symmetries, were imposed; but in three-body processes the sign difference does show up! Also difference in the two-body amplitudes responsible for the final state interaction was found to be visible in the break-up channels, so the data could be used to discriminate different two-body models used. In both works the authors also calculated the K^-d scattering length A_{K^-d} . The best value obtained for this quantity in those works may be identified as $(-1.34 + i 1.04)$ fm [15].

The third multi-channel three-body calculation was carried out in Refs. [16, 17] for low energy elastic K^-d scattering as well as to find the best theoretical value for A_{K^-d} . The data used to the χ^2 -fits to determine the two-body separable interactions were the same as in [15]. The novelty was to use relativistic formalism, hence the correct kinematics was ensured when dealing with different total masses (or different thresholds) in the entrance and exit channels, both in two-body input amplitudes as well as in three-body coupled equations. With the 3D_1 partial wave component included in the deuteron channel interaction, the best value was $A_{K^-d} = (-1.51 + i 1.45)$ fm.

After the last theoretical calculation just discussed above had come out in 1990 [16], the low energy $\bar{K}d$ physics became dormant for about ten years. One may identify some of the possible reasons for that void:

(i) *The kaonic hydrogen puzzle* mentioned earlier kept persisting, so it was felt that without any solution to it, one could not find any credible low energy K^-p amplitude for use to improve K^-d models.

(ii) The rank one separable potentials adopted to model the essential ingredients, namely the coupled $\bar{K}N$ - πY amplitudes, lacked support from underlying strong interaction theory. So, even by adopting isospin symmetry to fit the existing data, there was no compelling reason to believe that the *best fitting amplitudes* be really acceptable on

physical ground (a serious attempt of this type dated back to Henley *et al.* and Fink *et al.* [20]). In this respect some efforts to constrain the fitting parameters by $SU(3)$ symmetry deserve to be noted [21, 22]. However, the separable ansatz still needed to be given a proper justification. It should be useful to note that there were also local versions of the corresponding potentials based upon physical constants from Chiral Lagrangian to be somewhat tuned [23], but the local form had no support from the supposedly more fundamental theory, either. In addition to this, taking into account the isospin breaking effects would have pushed the picture farther into the mist. So why should one go forward under such circumstances?

Quite fortunately, there were two major breakthroughs: one on the experimental and the other on the theoretical front.

First, the long haunting *kaonic hydrogen puzzle* was finally put to an end by the KEK experiment [24], and the K^-p scattering length $a_{K^-p}^c$, where Coulomb effects are not separated, was extracted to be: $a_{K^-p}^c = (-0.78 \pm 0.15(stat) \pm 0.03(syst)) + i(0.49 \pm 0.25(stat) \pm 0.12(syst))$ fm, by applying the Deser-Trueman formula [25] to the kaonic hydrogen $1s$ level shift Γ , and width ϵ , by K^-p strong interaction :

$$\epsilon + i\frac{\Gamma}{2} = 2\alpha^3 \mu^2 a_{K^-p}^c,$$

with α the fine structure constant and μ the K^-p reduced mass. Although the thus obtained quantity includes the effect of the Coulomb interaction, hence not identical to the corresponding quantity due exclusively to strong interaction, the difference is, even conservatively, at most within a few percent: in the case of pionic hydrogen the difference appears to be below 1%, see for example [26, 27], so the extracted $Re(a_{K^-p}^c)$ finally was found to have the same sign as the one from the analysis of scattering data. The DEAR project [28] with the *DAΦNE* facility (ϕ -factory) at Frascati had been planning to repeat the experiment with higher precisions, and the data taking is reported to have been over. In addition, along with other experiments involving various K -mesons, this project has planned to measure the corresponding quantities for the K^-d atom, and the experiment is expected to start soon [29]. To obtain the K^-n scattering length without recourse to isospin symmetry (hence to find out how good that symmetry is realized in the kaon sector in this quantity) is one of the objectives for this measurement. But, a more ambitious picture such as using the quantities obtained to extract the kaon-nucleon Sigma-term: σ_{KN} , with the help of theories such as Chiral Perturbation Theory, see for example Ref. [30], has been some strong driving force for the experiment [4, 31, 32]. In fact, such a program has been put into practice recently using the pionic hydrogen and deuterium [33]. It should be useful to mention here that extracting the *Coulomb corrected* K^-d scattering length through the Deser-Trueman formula may not be as accurate as that for the K^-p system, and that relation between the purely strong and Coulomb corrected K^-d scattering length may not be quite simple either. This was discussed in terms of simple models by Barrett and Deloff [34], see also [26]. This will be revisited in Section V .

Second, based upon chiral perturbation theory, there has been a steady progress in describing the low to medium energy meson-baryon interaction. And within the context of our present interest, there was an important breakthrough made by Oset and Ramos in describing the coupled meson-baryon channel amplitudes for the $S = -1$ sector [5]. The channels involved are: $\bar{K}N$, πY , and ηY . The driving (potential) terms to the two-body coupled Bethe-Salpeter equations were taken from the lowest order in the effective chiral Lagrangian for the 0^- octet mesons and $1/2^+$ octet baryons. Then, an on-shell ansatz developed in [35] was introduced, which enabled the authors to transform the coupled integral equations into a set of algebraic equations where the major task was to deal with the integration of various meson-baryon two-particle propagators which are ultra-violet divergent. With only two parameters adjusted to very plausible values, the cut-off at $p = 630$ MeV/c in the momentum integrations to be convergent, and the average octet meson decay constant set as $f = 1.15f_\pi$, the authors were able to reproduce various low energy data associated with the above-mentioned coupled channels impressively (the isospin breaking effect in the particle masses was included). Particularly, the $\Lambda(1405)$ was generated dynamically as an unstable bound state of K^-p in the $I = 0$ channel whose decay into πY was also correctly reproduced. As will be discussed in the next Section, what made this approach particularly noteworthy is that the on-shell ansatz they adopted turned out to be interpreted as a practical justification for a separable representation of two-body meson-baryon potentials, where coupling strengths are the product of two parts, one dictated by $SU(3)$ symmetry, the other depending on energy. Note that this on-shell ansatz was made to be rewritten in a more elegant form, viz. in the so-called N/D representation, or cast into a once-subtracted dispersion integral representation of the two-particle propagators, etc. There, the dynamical left-hand cut contributions were shown to be weak, and the divergent integrals were made finite by an introduction of several subtraction constants adjusted to reproduce the relevant data, including the $K\Xi$ channel [36–40].

Now, upon witnessing the experimental and theoretical progress reviewed above, the time is ripe for starting the K^-d scattering study again. In fact, the Oset-Ramos result [5] was applied to calculate the scattering length A_{K^-d} within what is called the fixed center (or fixed scatterer) approximation (FCA) by Kamalov et al. [41]. Here we want to claim that a more refined approach should match the Oset-Ramos type amplitudes. More specifically, we think it

necessary to exploit a reliable method in dealing with three-body scattering.

In this article, we thus present a complete study of the K^-d scattering length within the Faddeev equations. In Sec. II A we first adopt the approach due to reference [5] and construct the coupled s -wave separable $\bar{K}N$ interactions, including the coupling to the charge exchange, as well as the πY and ηY channels. We study different models, with parameters fitted to the available experimental data, along with the constraint to remain close to the SU(3) values. The results are presented both in the *isospin* and *particle* bases where the latter takes into account the isospin breaking effect in terms of the physical meson and baryon masses. The parametrizations chosen for the deuteron channel are described in Sec. II B. Then we discuss other two-body interactions adopted in our study in Sec. II C. In Section III, we review the structure of the relativistic three-body Faddeev equations. In Sec. IV, we calculate the K^-d scattering length by solving those equations, both in isospin and particle bases. To our knowledge, this is the first calculation done in the particle basis, permitting to evaluate the isospin breaking effects at the three-body level. The sensitivity of A_{K^-d} to the two-body input is investigated. The discussion is developed in Sec. V, and our conclusions are given in the last Section.

II. TWO-BODY INTERACTIONS

In this part, we describe the various two-body interactions used as input in the three-body equations. In the first two Subsections, we present the $\bar{K}N$ and NN interactions, which are the fundamental ingredients to the K^-d problem. The last Subsection is devoted to a brief description of the πN and YN interactions.

A. $\bar{K}N$ INTERACTIONS

Here, we intend to construct two-body coupled channel $\bar{K}N$ interactions. The coupled channels involved are $\bar{K}N$, πY , and ηY ($Y = \Lambda, \Sigma$) with different total charge states for the mesons and baryons (in the particle basis), or in different total isospin states (in the isospin basis). See Appendix A for the relation between those two representations. The physical masses used in the particle basis and average masses used in the isospin basis may be found in Table I.

1. Separable models

Let us use i, j, k, \dots , etc. as channel indices. Since our present interest is in the $\bar{K}p$ near its threshold, we may safely assume that any given meson-baryon system in the coupled channel is in the relative orbital angular momentum s -state ($\ell = 0$). So we may adopt the s -wave projected coupled Bethe-Salpeter (or relativistic Lippmann-Schwinger) t -matrix equations [42] for the transition $j \rightarrow i$ which takes the following form:

$$T_{ij} = V_{ij} + \sum_k V_{ik} G_0^k T_{kj}, \quad (1)$$

where V_{ij} is the transition potential, and G_0^k is the free meson-baryon propagator for the intermediate channel k . We note here that implicit in the above expression are that (i) the meson-baryon systems are in the center of mass frame, and (ii) the integration is performed over the off-shell four momentum associated with channel k .

We take two additional simplifications to make the coupled equations manageable. The first one is to adopt the Blankenbecler-Sugar procedure to reduce the momentum integration from four to three dimensions [43–45]. In particular, the two-particle propagator is re-expressed as $G_0^k = G_0^k(p_k; \sigma)$, where p_k is the magnitude of the three-dimensional relative momentum of the intermediate channel k , and σ is the square of the total center of mass energy. This may be done by taking the discontinuity of G_0^k over the unitarity branch cut and use it to represent G_0^k in a dispersion integral form. We note that this procedure results in on mass shell but off energy shell form of equations which may be regarded as a relativistic extension from a familiar non-relativistic scattering theory. The second simplification step is to assume that the s -wave potentials take a non-local separable form:

$$V_{ij}^I = g_i(p_i) \lambda_{ij}^I(\sigma) g_j(p_j), \quad I = 0, 1, \quad (2)$$

where I is the total isospin for the meson-baryon system, and g_i is the cut-off form factor for channel i which is assumed to be a function of the magnitude of the three dimensional relative momentum vector in the same channel. In general the coupling strength λ_{ij}^I is assumed to be a function of σ as indicated in the above equation with no

left-hand cut assumed. Some rudiments of how our coupled two-body t -matrices may be obtained with the separable interactions is found in Appendix B.

Now, when we compare the expression for the coupled $\bar{K}N$ channel t -matrices, Eq. (20) in [5] with our coupled channel t -matrices, T_{ij} Eq. (B6) for which the related quantities are defined in Eqs. (B7, B8), we see immediately that the two results are identical provided that (i) we set $g_i(p_i) \equiv 1$ for all i , (ii) impose a momentum cut-off p_{max} in the integration in Eq. (B8), and (iii) set

$$\lambda_{ij}^I \equiv -C_{ij}^I \frac{1}{4f^2} (\epsilon_i + \epsilon_j). \quad (3)$$

The expression for λ_{ij}^I above is from Oset and Ramos [5], which was obtained from the lowest order expansion in $1/f$ of the chiral Lagrangian for the octet 0^- mesons coupled to the octet $1/2^+$ baryons. The coefficients C_{ij}^I are due to $SU(3)$ symmetry and tabulated as: $C_{ij}^{I=0} = D_{ij}$, $C_{ij}^{I=1} = F_{ij}$ in that publication. These are convenient for the isospin basis, but may be trivially transformed to the corresponding coefficients C_{ij} (for K^-p) and \tilde{C}_{ij} (for the K^-n related channels), for use in particle basis, also tabulated in [5]. The corresponding change to obtain the strength parameters in the particle basis in terms of the λ_{ij}^I follows trivially, see for example Eq. (A2). In our equation (3) above, ϵ_i and ϵ_j are the meson energies in the centre of mass system for the i and j channels, respectively.

Though our argument above went just in the opposite direction to what one finds in Oset and Ramos [5] (see also a more formally trimmed version of the Oset-Ramos line of derivation by Nieves and Arriola [38]), we have established a practical equivalence between the separable potential and the on-shell ansatz for the coupled meson-baryon equations. So within the framework of effective meson-baryon field theory, it is now possible to claim that the separable ansatz is a very reasonable starting point in describing the s -wave interactions at low energies. In our present work we choose to retain the form factors rather than imposing a sharp cut-off. This is due to the fact that when solving the three-body equations we rotate the momentum integration path off the real axis and into the complex plane. For that purpose, a sharp cut off is not practical. Then in order to respect $SU(3)$ symmetry, we choose to use a single form factor for all the different channels with a monopole form:

$$g(p) = \frac{\beta^2}{p^2 + \beta^2}, \quad (4)$$

where β is the effective cut-off momentum. Based upon the discussion above we adopt two slightly different types of interactions. The first one which we call OS1 is just V_{ij}^I , Eq. (2), with $g_i = g_j \equiv g(p)$, and λ_{ij}^I from Eq. (3). We expect this interaction to produce a very similar result to the original Oset and Ramos [5] model. The second interaction model is called OSA, which is a variant of OS1 in that it incorporates the possible $SU(3)$ breaking effect in the coupling strengths (or in the meson decay constant f) in terms of extra parameters b_{ij}^I with the substitution: $C_{ij}^I \rightarrow b_{ij}^I C_{ij}^I$. We then adjust on the relevant data β , f , and b_{ij}^I 's, the last ones only for OSA, with a constraint that the $SU(3)$ breaking effect is reasonably contained.

It is important to stress here that we follow the observation by Oset and Ramos [5] and retain the ηY channels in our fit although this channel has a substantially higher threshold as compared with that for $\bar{K}N$, see Table I. The necessity for the inclusion of these channels will be demonstrated later. As a result we have three coupled channels: $\bar{K}N$, $\pi\Sigma$, $\eta\Lambda$ to deal with for $I = 0$, and four coupled channels: $\bar{K}N$, $\pi\Sigma$, $\pi\Lambda$, $\eta\Sigma$ for $I = 1$. In terms of physical (or particle) channels the following two groups are separately coupled:

$$K^- p \rightarrow K^- p, \bar{K}^0 n, \Lambda\pi^0, \Sigma^+\pi^-, \Sigma^0\pi^0, \Sigma^-\pi^+, \Lambda\eta, \Sigma^0\eta, \quad (5)$$

$$K^- n \rightarrow K^- n, \Lambda\pi^-, \Sigma^0\pi^-, \Sigma^-\pi^0, \Sigma^-\eta. \quad (6)$$

Below in the next Subsection we briefly review available experimental data to which the model interactions are fitted and compared.

2. Experimental data

Since there are no data associated with the initial K^-n channels in Eq. (6), we only discuss the ones in Eq. (5). Furthermore, in the low energy range of our current interest, *i.e.* $p_K^{lab} \leq 250$ MeV, the last two channels involving

the η meson are physically closed as their thresholds are substantially higher than the rest. Otherwise the remaining physically accessible coupled channels are now strongly influenced by the $I = 0$ $\Lambda(1405)$ resonance below the K^-p threshold which decays almost exclusively to $\pi\Sigma$. Note also that while the $\bar{K}^0 n$ has a slightly higher threshold, all the πY channels have lower threshold than that for K^-p . So altogether there is a very rich structure in this coupled set of channels ¹. In the energy range considered here, some 90 data points are available [46–54]. These data, obtained between 1965 and 1983, bear unequal accuracies, as briefly discussed later.

Moreover, accurate data [48, 49, 55–57] for threshold branching ratios are also available, *i.e.*,

$$\gamma = \lim_{k \rightarrow 0} \frac{\Gamma(K^-p \rightarrow \pi^+\Sigma^-)}{\Gamma(K^-p \rightarrow \pi^-\Sigma^+)} = 2.36 \pm 0.04, \quad (7)$$

$$R_c = \lim_{k \rightarrow 0} \frac{\Gamma(K^-p \rightarrow \text{charged particles})}{\Gamma(K^-p \rightarrow \text{all final states})} = 0.664 \pm 0.011, \quad (8)$$

$$R_n = \lim_{k \rightarrow 0} \frac{\Gamma(K^-p \rightarrow \pi^0\Lambda)}{\Gamma(K^-p \rightarrow \text{all neutral states})} = 0.189 \pm 0.015. \quad (9)$$

There are also data [58] on the invariant mass spectrum of the $\Sigma^+\pi^-$ system, which have been exploited to investigate the nature of the $\Lambda(1405)$ resonance.

Finally, the last piece of crucial experimental information comes from the recent KEK measurement [24] of the K^-p scattering length. As explained in the Introduction, the obtained value which includes the Coulomb effect: $a_{K^-p}^c = (-0.78 \pm 0.15 \pm 0.03) + i(0.49 \pm 0.25 \pm 0.12)$ fm, resolves the "kaonic hydrogen puzzle".

3. Results of the fit

For model OS1 interaction, we have adopted the same strategy as in Ref. [5] by fitting our parameters f and β to the threshold branching ratios, with f constrained to deviate from f_π by less than $\pm 20\%$. All other observables are "predicted", *i.e.* they are evaluated with the values of the parameters reached at the end of minimization (these values can be found in Ref. [1]). The branching ratios and the a_{K^-p} scattering length obtained in this model are comparable to the values from the Oset-Ramos model, see Table II. The same conclusion holds when we compare the total cross sections and the $\pi\Sigma$ mass spectrum given in Figs. 1 and 2 with the corresponding results in Ref. [5].

For the OSA interaction, the parameters are f , β , and b_{ij}^I 's, which are fitted to the threshold branching ratios and the K^-p initiated cross sections, with the b_{ij}^I 's constrained to remain within $\pm 30\%$ of their exact $SU(3)$ -symmetry values. The obtained values are given in Table III ². Note that in the lowest order chiral Lagrangian approach, some coupling coefficients: $C_{ij}^{I=0} = D_{ij}$, $C_{ij}^{I=1} = F_{ij}$ as found in Tables 2 and 3 in Ref. [5] are equal to zero. We have chosen to keep these zero values, thus we do not need the corresponding $SU(3)$ breaking coefficients b_{ij}^I , which is reflected in Table III.

Our results for OSA are presented in Table II and Figs. 1, 2 along with available data as well as values from a few earlier models. We first discuss the result for K^-p initiated channels in the particle basis. As shown in Table II, the threshold reaction ratios: γ , R_c , R_n are better reproduced by OSA than by OS1. Regarding the K^-p scattering length, our result is a prediction since we have not used the value extracted from the kaonic hydrogen atom [24] as part of the constraint in the fitting procedure. The real part is obtained closer to the data [24] by OSA than by OS1. As for the imaginary part, both models give the values at the limit of the experimental uncertainties within 2 standard deviation. We point out that this trend for $\text{Im}(a_{K^-p})$ is systematically observed with either the present separable models or with the Oset-Ramos approach. The cross sections are also better reproduced with OSA than with OS1, see Fig. 1, especially those for the $K^-p \rightarrow \pi^-\Sigma^+$ and the $K^-p \rightarrow \bar{K}^0 n$ channels which now have the correct magnitude as compared with the data. The position of the $\Lambda(1405)$ resonance predicted by the present models are quite similar, and in good agreement with the data, see Fig. 2 (and also Fig. 4). Finally, we have calculated the

¹ Notice that the contributions from the $K^-p \rightarrow K^0\Xi^0$, $K^+\Xi^-$ channels, which couple only indirectly to the $\bar{K}N$ system, were found insignificant [5] at low energies, and hence are not included in our formalism. Moreover, our aim in this work being to use the elementary reactions as input in the K^-d elastic scattering, the electromagnetic processes $K^-p \rightarrow \Lambda\gamma$, $\Sigma^0\gamma$, studied by other authors [21, 22], are not considered here.

² In our previous publication [1], interaction OS2 was introduced which took an identical form to the current OSA. The resulting fits by these two models are very similar. The major difference is that the $SU(3)$ breaking has come out less in OSA than in OS2, due to a more careful handling of the data-base.

cross section of the $K^-p \rightarrow \eta\Lambda$ reaction near threshold. We have found that the results predicted by models OSA and OS1 are in reasonable agreement with the recent data [59] from the Crystal Ball detector at Brookhaven: the steep rise just above the threshold, and the s -wave behavior expected for pseudoscalar meson production at threshold, are correctly reproduced.

As for the results obtained in the isospin basis we only discuss the case with the OSA interaction, as the characteristic feature is the same with the result from the OS1 interaction. Here, we use the average masses of the hadron isospin multiplets everywhere (see Table I), hence now, for example, the charge exchange reaction: $K^-p \rightarrow \bar{K}^0 n$ becomes elastic energy-wise. Note that to calculate reaction cross sections, the entrance channel energies are taken using the physical particle masses, which are also used to find the final state phase space volumes. In Table II, we observe large differences between the values of the threshold ratios γ and R_n calculated in the two bases. The shift of the cusps in the cross sections when using the isospin basis are clearly exhibited in Fig. 1. On the contrary, the position of the $\Lambda(1405)$ resonance is only slightly affected. These differences between the results in the two bases are similar to those observed in Ref. [5].

Next we study the effect due to the contribution from the ηY channels. Given that the difference between the two thresholds for $\eta\Lambda$ and K^-p final states is as large as ~ 230 MeV (with $\eta\Sigma$ the difference is about 75 MeV larger), hence *a priori* the effect from the coupling to these channels is expected to be insignificant. However, in Ref. [5] the authors observed the importance of retaining these channels. So we want to check their claim. Very qualitatively, the role of these channels may be best understood in the exact isospin symmetry limit. Then ηY channels are the only ones whose thresholds are above the one for the $\bar{K}N$. Hence, they provide a definite attraction to the elastic $\bar{K}N$ process. As a result the coupling to ηY states controls the binding properties of the $\bar{K}N$ (in the effective chiral interaction adopted here, the $I = 0$ $\Lambda(1405)$ is a bound state of $\bar{K}N$ embedded in the continuum state of the $\pi\Sigma$ channel). As a first step, we have discarded these channels from model OSA by forcing the $\bar{K}N$ - $\eta\Lambda$ and $\bar{K}N$ - $\eta\Sigma$ strengths to zero, without changing other parameters. Then, we have recalculated the amplitudes and observables. This model will be hereafter referred to as "OSA, ηY excluded". The results are given in Table II and Fig. 1. The only observables which are not affected are the threshold ratio R_c and the $K^-p \rightarrow \pi^+\Sigma^-$ cross section. All other quantities are significantly modified, especially γ and R_n as well as the $K^-p \rightarrow \bar{K}^-p$ and $K^-p \rightarrow \pi^-\Sigma^+$ cross sections which become unrealistic. Also, the maximum of the $\pi\Sigma$ mass spectrum is shifted towards the higher values of the momentum, thus incompatible with the data. Similar effects have been pointed out in Ref. [5]. This situation can be understood by examining the values of the strength parameters in Table III. The $\bar{K}N$ - ηY strengths deviate from unity by about 15% to 25%, and it is not possible to obtain a correct overall fit if they are constrained to stay closer to unity (in particular, the position of the $\Lambda(1405)$ resonance is not correctly reproduced). This does indicate that the $\bar{K}N$ - ηY strengths take part in the minimization procedure at about the same level of importance as the other ones, and it is meaningless to turn them off entirely without re-adjusting other parameters. In order to see this problem from a somewhat different angle we have introduced yet another model: OSB, a variant of OSA in which the ηY channels are excluded from the beginning. The values of the parameters are given in Table III. The results obtained for the K^-p branching ratios and scattering length are close to those obtained with OSA, see Table II. This is also the case for the total cross sections. However, the position of the $\Lambda(1405)$ resonance is now shifted towards lower values of the momentum, see Fig. 2, which means that OSB is not able to reproduce the properties of the $\Lambda(1405)$. We thus need to retain the ηY channels.

Lastly, we use the parameters thus obtained both for OS1 and OSA to calculate the amplitudes (or t -matrices) for the K^-n initiated processes, see Eq. (6), for which, as mentioned earlier, there is no data to be confronted with. We still need those amplitudes for our K^-d three-body calculations. Here along with the corresponding quantity in the K^-p initiated channels, we only present the scattering lengths as found in Table IV. The differences between the results given by two models do not exceed $\sim 30\%$. For comparison we give also the values obtained by Oset and Ramos [5]. Our OS1 results agree with those values within $\sim 15\%$, in line with the differences previously observed on the other observables. The symmetry breaking effect in the mass of the hadron isospin multiplets is quite visible, especially in the real parts, since in the limit of isospin symmetry, one has: $a_p = a_n^o$, and $a_{ex} = a_p - a_n$. Note that the scattering lengths in Table IV have been obtained at the K^-p threshold (except for the elastic K^-n process). In fact, these quantities are very sensitive to the value of the threshold at which they are calculated, which is then reflected in the values obtained for the A_{K^-d} scattering length. These aspects have been discussed in our previous paper [1], and will be revisited at beginning of Sec. IV.

In conclusion, the OS1 and OSA parametrizations are good candidates to be used in the three-body calculation. It is clear that such interactions, the parameters of which are determined by a fit to the available observables in the particle basis with the chiral SU(3)-symmetry constraint, must definitely be preferred to previous separable interactions with parameters determined in the isospin basis, without any symmetry constraint, as it was the case in Refs. [13–16, 20].

B. NN INTERACTION

We have considered three different relativistic separable potentials to describe the deuteron (d) channel. The structure of the equations may be read off from the coupled-channels cases described in Appendix B by replacing the particle labels with the angular momentum labels relative to the 3S_1 and 3D_1 coupled partial waves.

All the interactions considered are of rank-1. Characteristic to such potentials, the static parameters are correctly reproduced, namely: the triplet effective range parameters a_t and r_t , the D -state percentage value P_D , the quadrupole moment Q , and the asymptotic ratio $\eta = A_D/A_S$. On the other hand, the 3S_1 and 3D_1 phase shifts cannot be reproduced simultaneously.

The first model (hereafter called model A) is the one proposed in our work on the πd system [61], namely the parametrization denoted by $SF(6.7)$ therein, with $P_D = 6.7\%$. This model is an extension of the usual Yamaguchi-type interactions, using form factors which are expressed as ratios of polynomials. The parameters are fitted to the static properties, the 3S_1 phase shift, and also to the deuteron monopole charge form factor up to about 6 fm^{-1} . All details can be found in Ref. [61].

Besides this model fitted to on-shell properties only, we have considered a second model derived from the PEST1 potential constructed by Haidenbauer and Plessas in Ref. [62]. The authors have constructed a separable representation of the Paris potential to reproduce both its on-shell and off-shell characteristics. Among various NN partial waves, special care is devoted to the coupled 3S_1 - 3D_1 state. The best approximation to the Paris potential requires a rank-4 interaction. However, for applications where only the deuteron bound-state enters, a rank-1 parametrization was proposed, called PEST1, with all deuteron properties (including the wave functions) being practically the same as those given by the Paris potential. The price to pay is that the form factors are chosen as sum of rational functions, with many parameters, see Ref. [62]. As the PEST1 parametrization is non-relativistic, we have extended it by means of *the minimal relativity rule*. More specifically, the relativistic potential V^R between nucleons 1 and 2 is obtained from the non-relativistic one V^{NR} according to the following transformation in momentum space:

$$V^R(p, p') = (2\pi)^3 \sqrt{2\epsilon_{1p} 2\epsilon_{2p}} V^{NR}(p, p') \sqrt{2\epsilon_{1p'} 2\epsilon_{2p'}}, \quad (10)$$

with $\epsilon_{ip} = \sqrt{\mathbf{p}_i^2 + m_i^2}$ the total energy of nucleon i . Taking V^{NR} as separable: $V^{NR}(p, p') = \lambda g(p)g(p')$, $V^R(p, p')$ has the same form, with $g(p)$ multiplied by: $2\sqrt{(2\pi)^3} \sqrt{\mathbf{p}^2 + m^2}$. We have checked that this transformation induces only slight changes in the deuteron properties. For example, the original P_D value is 5.8%, and the value obtained after the relativistic transformation is 6.1%. So, we can keep the original parameters. In our present work this is denoted as model B.

Finally, in order to assess the importance of the D -state contribution in the low energy K^-d scattering, we have used a pure 3S_1 relativistic potential, with form factor as given in Eq. (4). The values of the strength and range parameters fitted to E_D and a_t are: $\lambda_d = -5974.2$, $\beta_d = 1.412 \text{ fm}^{-1}$, respectively. This model is called model C.

C. OTHER TWO-BODY INPUT

We have also considered the contributions of the πN - P_{33} and coupled YN interactions. As will be explained in Sec. IV C, these two-body channels start to contribute from the second order in the multiple scattering expansion of the Faddeev equations, so their contribution in the low energy K^-d observables is expected to be moderate or even small.

1. πN - P_{33} interaction

We have chosen a conventional Δ -isobar model where the Δ resonance is parametrized according to a one-term separable potential:

$$V(p, p'; \sigma) = g(p) \frac{\lambda_\Delta}{\sigma - m_0^2} g(p'). \quad (11)$$

Here, σ is the πN total c.m. energy squared, and m_0 the bare Δ mass. A p -wave monopole form factor is assumed with cut-off Λ :

$$g(p) = \frac{p}{p^2 + \Lambda^2}. \quad (12)$$

The strength parameter λ_Δ , together with m_0 and Λ , are fitted to the P_{33} phase-shift. In the relativistic approach, we have obtained the following values: $\lambda_\Delta = 218.582$, $m_0 = 1308.8$ MeV, and $\Lambda = 290.9$ MeV/c.

In order to solve the three-body equations in the particle basis, it is necessary to introduce different charge states of the pion and nucleon. So, the following states will contribute: the $(\pi^0 p, \pi^+ n)$ and $(\pi^- p, \pi^0 n)$ coupled states, and the $(\pi^- n)$ state. The corresponding separable two-body potentials are obtained by choosing the same form factors as Eq. (12) in all channels, and expressing the strength parameters in terms of λ_Δ , see Appendix A. The resulting two-body t -matrices entering the three-body equations are obtained straightforwardly.

2. YN interactions

The hyperon-nucleon interaction has been well studied in the past. One of the most popular approaches is meson-exchange potential models with $SU(3)$ symmetry constraints used in the coupled channels equations, see Ref. [63] and references therein. Besides, the intrinsic interest in investigating the available YN experimental data, these interactions serve as input to hypernuclear physics. Concurrently, separable models have been developed, and some of them have been used as input to K^-d three-body calculations. In particular, the effect of the final state YN interaction (limited to s -waves) on the Λp invariant mass distribution near the ΣN threshold was studied in Refs. [14, 15]. One of the main conclusion was that the best reproduction of the shoulder in the Λp mass spectrum favoured models which do not support an unstable ΣN bound state. The interactions that we have elaborated in Ref. [16, 17] and the one presented in this work fulfill this condition.

The data to which the adjustable parameters of the separable potential should be fitted are scarce and exhibit rather large error bars. To our knowledge, there are no new data in addition to those used in our previous work, namely: (i) the $\Sigma^+ p \rightarrow \Sigma^+ p$, $\Sigma^- p \rightarrow \Sigma^- p$, $\Sigma^0 n$, Λn , and $\Lambda p \rightarrow \Lambda p$ total cross sections, in the hyperon momentum range $p_Y^{lab} \leq 300$ MeV/c, (ii) the $\Sigma^+ p \rightarrow \Sigma^+ p$, $\Sigma^- p \rightarrow \Sigma^- p$, and $\Sigma^- p \rightarrow \Lambda n$ differential cross sections for $p_Y^{lab} \sim 300$ MeV/c. See Refs. [64–70].

In Refs. [16, 17], we have used most of these data to determine the parameters of two models: one non-relativistic, and the other relativistic. The calculations were done in the isospin basis, where one must consider the ΣN - ΛN ($I = 1/2$) coupled channels and the ΣN ($I = 3/2$) single channel. The main conclusion was that the total cross sections are dominated by the 3S_1 partial wave, except for $\Sigma^+ p \rightarrow \Sigma^+ p$ which is dominated by the 1S_0 wave, while the P and D partial waves have a significant contribution only in the $\Sigma^- p \rightarrow \Lambda n$ total cross section (of course, these higher partial waves must be taken into account if the differential cross sections are added to the data to be fitted).

The model used in the present study is an extension of the above mentioned relativistic model to calculate the observables in the particle basis. Only the 3S_1 partial wave contributions are included, thus the parameters are fitted to the total cross sections, except for $\Sigma^+ p \rightarrow \Sigma^+ p$. Note that neglecting the 1S_0 partial wave is justified in the three-body calculation at low energies, since the contribution from the singlet S -wave YN interactions is excluded for parity considerations. We take as adjustable parameters the coupling strengths and the ranges of the form factors in the isospin basis. The observables are calculated in the particle basis, where the following channels contribute: the $(\Sigma^0 p, \Sigma^+ n, \Lambda p)$ and $(\Sigma^- p, \Sigma^0 n, \Lambda n)$ coupled channels, and the $\Sigma^- n$ and $\Sigma^+ p$ single channels. The relations between the strengths parameters in the two bases can be found in Appendix A, and the transition matrices for the different reactions are obtained from the general expressions given in Appendix B. We take monopole form factors, Eq. (4), with isospin-independent ranges. The values of the fitted parameters are given in Table V, and the cross sections in Fig. 3. The selected data can be well reproduced by this simple model, but a large reduction effect is observed when isospin basis is adopted in the total cross sections for the $\Sigma^- p$ induced reactions at low values of the hyperon momentum. We give in Table VI the YN scattering lengths calculated in the particle basis. Except for $a_{\Sigma^+ p - \Sigma^+ p}$ and $a_{\Sigma^- n - \Sigma^- n}$ which are practically equal, the symmetry breaking effects are large. For example, at the limit of exact isospin symmetry, one should have: $a_{\Sigma^- p - \Sigma^0 n} = \sqrt{2}(a_{\Sigma^0 n - \Sigma^0 n} - a_{\Sigma^- p - \Sigma^- p}) = -a_{\Sigma^+ n - \Sigma^+ p} = \sqrt{2}(a_{\Sigma^0 p - \Sigma^0 p} - a_{\Sigma^+ n - \Sigma^+ n})$, which is clearly not the case.

III. THREE-BODY EQUATIONS FOR THE K^-d SYSTEM

In this Section, we describe the three-body equations for the K^-d system, in which the two-body input described in the previous Section will enter. In the first Subsection, we recall the general form of the three-body equations written in the isospin basis, in the case of coupled two-body input channels, and we give the equations for the rotationally

invariant amplitudes. Then, the antisymmetrization due to the identity of the two nucleons in the isospin basis is examined. In the second Subsection, the extension to the particle basis is given. Some important aspects concerning the practical calculation are considered in the third Subsection.

A. Three-body equations in the isospin basis

The extension of the usual three-body equations to the case where the two-body operators connect two states involving particles which are different (i.e. inelastic channels), results in the following system of coupled equations, written in operator form:

$$X_{ab}(s) = Z_{ab}(s) + \sum_{c,c'} Z_{ac}(s) R_{cc'}(s) X_{c'b}(s), \quad (13)$$

with s the 3-body total energy. Here, a, b, c and c' are the indices which specify the particles involved in the various three-body channels, namely the spectator and the interacting pair. X_{ab} is the transition amplitude between channels a and b , and Z_{ab} is the corresponding Born term. The main difference with respect to the usual case is that the two-body operator $R_{cc'}$ connects two different two-body states labeled as c and c' .

We now specify the values taken by the channel indices in Eq. (13). Taking into account all the two-body input considered in Section II, one must consider the following types of three-body channels in the isospin basis: $d[\bar{K}(NN)]$, $y[N(\bar{K}N)]$, $\alpha[N(\pi Y)]$, $\mu[N(\eta Y)]$, $\beta[\pi(YN)]$, and $\Delta[Y(\pi N)]$. Here, the first letter is the *label* of the channel, and in square braces we specify the *spectator* and the associated *pair* of particles. In fact, labels y , α , μ and β can be considered as "generic" names. In practice, extra indices are needed to fully describe the physical situation. For example, for the pairs corresponding to the $\bar{K}N$ interactions, there are three $I = 0$ coupled channels ($\bar{K}N-\pi\Sigma-\eta\Lambda$), and four $I = 1$ coupled channels ($\bar{K}N-\pi\Sigma-\pi\Lambda-\eta\Lambda$). A similar situation occurs in the case of the β channels corresponding to the $\Sigma N-\Lambda N$ ($I = 1/2$) coupled channels. The corresponding three-body channels are labeled as summarized in Table VII. Note that in channel Δ , the spectator hyperon Y is restricted to Σ , from isospin considerations.

In the formal equations (13), the channel indices a, b, c, c' take their values in the set defined above: $\{d, y, \alpha, \mu, \beta, \Delta\}$, and the different quantities: X, Z, R , can be considered as matrices with respect to these indices.

The transitions between different two-particle states are induced by the two-body operators $R_{cc'}$: for example, $R_{y\alpha}$ is the quantity $R_{\bar{K}N-\pi Y}$ corresponding to the two-body t -matrix for the $\bar{K}N \rightarrow \pi Y$ transition, evaluated in the presence of a spectator nucleon. Written in matrix form, the non-vanishing R operators appear as block-matrices as shown in Table VIII.

Concerning the Born terms, only those which connect initial and final states involving the same three particles are different from zero. These terms are shown in matrix form in Table IX. For example, Z_{dy} is the Born term for the exchange of a nucleon between the $\bar{K}(NN)$ and $N(\bar{K}N)$ states. Note that Z_{dd} is equal to zero, since no particle can be exchanged between the initial and final NN pairs. We note also that, using the two-body input channels considered here, there is no Born term involving an ηY pair. To have such terms, it would be necessary to take into account the contributions of three-body channels like $\eta(YN)$, $Y(\pi N)$ and $Y(\eta N)$. (the last two channels necessitate to introduce the $\pi N-\eta N$ two-body coupled system). These contributions are expected to be negligible at the K^-d threshold.

The successive steps leading from the formal equations (13) to the relativistic equations for the rotationally invariant amplitudes are the same as in the usual case. We refer the reader to References [17, 44, 45, 71, 72] for all details. The final equations read:

$$X_{\tau_a \tau_c}^{\mathcal{J}\mathcal{I}}(p_a, p_c; s) = Z_{\tau_a \tau_c}^{\mathcal{J}\mathcal{I}}(p_a, p_c; s) + \sum_{b, \tau_b; b', \tau_{b'}} \int \frac{dp_b p_b^2}{2\epsilon_b} Z_{\tau_a \tau_b}^{\mathcal{J}\mathcal{I}}(p_a, p_b; s) R_{b b'}^{c_b = c_{b'}}(\sigma_b) X_{\tau_{b'} \tau_c}^{\mathcal{J}\mathcal{I}}(p_b, p_c; s), \quad (14)$$

where σ_b is the invariant energy of the pair in channel b expressed in the three-body center of mass system, $c_a = (J_a, S_a, I_a)$ specifies the conserved quantum numbers of the pair in channel a , and $\tau_a = (c_a, l_a, \Sigma_a)$ specifies the three-body quantum numbers in this channel. Note that labels c and τ refer to the spin-isospin variables in a given channel. For example, assuming that channel a is composed with particle i as spectator and the pair (jk) , we define the following quantities:

- \mathbf{s}_i : spin of particle i ,
- $\mathbf{S}_i (= \mathbf{s}_j + \mathbf{s}_k)$, \mathbf{L}_i , and $\mathbf{J}_i (= \mathbf{L}_i + \mathbf{S}_i)$: spin, orbital angular momentum, and total angular momentum, respectively, of pair (jk) ,
- $\mathbf{\Sigma}_i (= \mathbf{s}_i + \mathbf{J}_i)$, l_i , and $\mathcal{J} (= l_i + \mathbf{\Sigma}_i)$: channel spin, orbital angular momentum of i and (jk) , and three-body total angular momentum, respectively.

The isospin variables are defined in the same way:

- \mathbf{t}_i : isospin of particle i ,
- $\mathbf{I}_i (= \mathbf{t}_j + \mathbf{t}_k)$: isospin of pair (jk) ,
- $\mathcal{I} (= \mathbf{t}_i + \mathbf{I}_i)$: three-body total isospin.

The notations used in Eq. (14) for the two-body propagators are the following: the lower indices b and b' refer to the involved coupled channels, and the upper "index" $c_b = c_{b'}$ means that the spin-isospin quantum numbers are conserved by the interaction, i.e.: $J_b = J_{b'}$, $S_b = S_{b'}$, $I_b = I_{b'}$ (the latter equality holds only in the isospin basis). For the uncoupled propagators, the single index c_b specifies completely the interacting pair.

The two-body propagators are calculated as explained in Section II and Appendix B, and the general expression of the Born term can be found in Refs. [17].

We end this Subsection with two specific aspects concerning the calculation of the Born terms in the isospin basis. The first one concerns the problem of antisymmetrization. In the isospin basis, the particles in the different multiplets are considered as identical. In particular, the neutron and proton are treated as identical particles: the nucleon N . Therefore, one must properly antisymmetrize the amplitudes and Born terms where the initial and final three-body states involve two nucleons. As a result, one must introduce antisymmetrization coefficients as explained in Appendix C. The second aspect concerns the problem relative to the "ordering" of particles when evaluating the Born terms. For example, let us consider the Z_{yy} Born term for \bar{K} exchange between two $\bar{K}N$ states, with a spectator nucleon. The antisymmetrized expression is, according to Appendix C:

$$\tilde{Z}_{yy} = -Z_{y^1y^2} = -\langle N_2(\bar{K}N_1) | G_0 | N_1(\bar{K}N_2) \rangle, \quad (15)$$

with G_0 the three-body propagator. Usually, the expressions given for the Born terms assume a cyclic ordering of the particle labels, see for example Refs. [17, 73]. Namely, one calculates for example: $Z_{ij} = \langle i(jk) | G_0 | j(ki) \rangle$, for the exchange of particle k between pairs (jk) and (ki) , where i, j, k are assumed to be cyclically ordered both in the initial and final states. In the case of $Z_{y^1y^2}$, Eq. (15), the spectator particles in the initial and final states are labeled as: $N_2 = i$, $N_1 = j$, thus the Born term has the "non-cyclic" form: $\langle i(kj) | G_0 | j(ki) \rangle$. We obtain the cyclic form by exchanging particles j and k (i.e. N and \bar{K}), in the pair of the final state. This introduces the following phase coefficient:

$$(-1)^{L_{\bar{K}N}} (-1)^{S_{\bar{K}N} - s_N - s_{\bar{K}}} (-1)^{I_{\bar{K}N} - t_N - t_{\bar{K}}}. \quad (16)$$

The first factor is due to changing the direction of the relative momentum of the pair, and the second (third) factor results from the property of the Clebsch-Gordan coefficients when the coupling order of the spins (isospins) of two particles is changed.

B. Extension to particle basis

In the particle basis, we consider the deuteron as composed of two distinct particles: the neutron (n) and the proton (p), and the particles of the different multiplets take their physical masses. The number of three-body channels to be considered increases considerably as compared to the isospin basis case. For example, we have seen in Section II A that for the $\bar{K}N$ interactions in the particle basis, we must consider the coupled channels related to K^-p , namely: $K^-p, \bar{K}^{\circ}n, \pi^-\Sigma^+, \pi^+\Sigma^-, \pi^{\circ}\Sigma^{\circ}, \pi^{\circ}\Lambda, \eta\Sigma^{\circ}, \eta\Lambda$, and those related to K^-n : $K^-n, \pi^-\Sigma^{\circ}, \pi^{\circ}\Sigma^-, \pi^-\Lambda, \eta\Sigma^-$. So, if we retain only these contributions in addition to the deuteron, the three-body channels to be considered are: the $K^-(pn)$ channel, the eight above channels with the neutron as spectator, and the five remaining channels with the proton as spectator. So, we have a 14×14 Born terms matrix. However, the number of non-zero Born terms is very limited. In the case considered here, we have only the following different Born terms: $\langle K^-(pn) | G_0 | n(K^-p) \rangle$ (proton exchange between the deuteron and the (K^-p) pair), $\langle K^-(pn) | G_0 | p(K^-n) \rangle$ (neutron exchange between the deuteron and the (K^-n) pair), $\langle n(K^-p) | G_0 | p(K^-n) \rangle$ (K^- exchange between the (K^-p) and (K^-n) pairs), $\langle n(\bar{K}^{\circ}n) | G_0 | n(\bar{K}^{\circ}n) \rangle$ (\bar{K}° exchange between the initial and final $(\bar{K}^{\circ}n)$ pairs), and the symmetric terms.

The matrix of propagators has a block structure similar to that in the isospin basis (Table VIII): single term for the deuteron propagator, 8×8 matrix for the channels coupled to K^-p , and 5×5 for the channels coupled to K^-n .

If we take into account the contributions of the πN and YN interactions, the following additional three-body channels must be considered (see Section II C): $\{\Sigma^-(\pi^{\circ}p), \Sigma^-(\pi^+n)\}$, $\{\Sigma^{\circ}(\pi^-p), \Sigma^{\circ}(\pi^{\circ}n)\}$, and $\Sigma^+(\pi^-n)$, coming from the πN interaction, and: $\{\pi^-(\Sigma^+n), \pi^-(\Sigma^{\circ}p), \pi^-(\Lambda p)\}$, $\{\pi^{\circ}(\Sigma^-p), \pi^{\circ}(\Sigma^{\circ}n), \pi^{\circ}(\Lambda n)\}$, and $\pi^+(\Sigma^-n)$, coming from the YN interactions.

The derivation of the equations for the rotationally invariant amplitudes, and the calculation of the Born terms, are done along the same lines as in the isospin basis. The main difference is that there is no problem relative to antisymmetrization, except for $\langle n(\bar{K}^{\circ}n) | G_0 | n(\bar{K}^{\circ}n) \rangle$ which must be antisymmetrized with respect to the two identical neutrons, as in the case of the Z_{yy} Born term calculated in the isospin basis, see Appendix C. Another important difference concerns the isospin dependence. In the isospin basis, the expression of the Born term involves a "6-j" coefficient originating from the transformation from initial to final three-particle isospin states, see Ref. [17, 73]. This coefficient depends on the values of the particle isospins, total isospin of the initial and final pairs, and three-body total isospin. In the particle basis, the individual isospins of all particles are well defined, but not the total isospin of the pairs (consequently, the c labels in Eq. (14) do not depend on the isospin I of the pairs). As the initial and final three-body states involve the same three particles, the isospin coefficient simply reduces to unity.

C. Practical calculation

For the practical calculation, we must first define the values of the various isospins, spins and angular momenta. At first, we consider the isospin basis case. The total isospin of the K^-d system is $\mathcal{I} = 1/2$. Now, in a given three-body channel, the quantum numbers (L, S, J, I) of the pair and the spin s of the spectator particle are fixed. The channel spin Σ is then given by: $|s - J| \leq \Sigma \leq s + J$, and the angular momentum l of the spectator relative to the pair by: $|\mathcal{J} - \Sigma| \leq l \leq \mathcal{J} + \Sigma$, with \mathcal{J} the three-body total angular momentum. For a given value of \mathcal{J} , the possible values of l can be ordered in two sets corresponding to opposite parities of the three-body system. The situation is summarized in Table X.

In the present paper, we consider only the K^-d scattering length which is defined as:

$$A_{K^-d} = - \lim_{p_K \rightarrow 0} \frac{1}{32\pi^2 \sqrt{s}} X_{dd}, \quad (17)$$

where X_{dd} is the ($\mathcal{J} = 1^-, l = l' = 0$) partial amplitude for K^-d elastic scattering, evaluated at the zero limit for the kaon momentum. If we retain the contributions of the $d+\bar{K}N+\Delta+YN$ two-body channels, we have a system of 12 coupled three-body channels (see Table VII). After angular momentum reduction, we obtain for $\mathcal{J} = 1^-$ a system of 25 coupled equations, see Table X. The singularities of the kernel ZX are avoided by using the rotated contour method [10], and, after discretization of the integrals, this system is transformed into a system of linear equations.

It is well known that the iterated form of the three-body equations does not converge. This is illustrated with the following results obtained (in the isospin basis) with the "OSA+deuteron-A" model. The values of A_{K^-d} obtained at first, second and third order of iteration are respectively (in fm): $(0.303 + i 3.258)$, $(-0.572 + i 3.684)$, and $(-1.366 + i 4.131)$, which clearly do not converge. To obtain the exact value, we solve the linear system by matrix inversion. In the above example, we get: $(-1.636 + i 2.618)$ fm. We can also use the Pade approximants technique which leads to a convergent solution from the successive iterated terms. In practice, we have used a diagonal [5/5] Pade (constructed with the 11 first iterates), which was found to be sufficient to achieve convergence. The dimension of the matrix to be inverted is rather large, especially when the contributions of the "small" two-body partial waves are taken into account. However, this is a sparse matrix because of the limited number of non-zero Born terms. Thus, it is much less time consuming to solve the linear system with using the Pade approximants method.

The extension to the particle basis case is straightforward. As explained above, in this case the Pade approximant method must be even more preferred to the usual methods for solving the linear system, since the number of coupled channels is much larger than in the isospin basis for a given choice of two-body contributions, but with a large number of Born terms equal to zero.

Note also that we have checked that, using the particle basis computer program with the particle masses in the multiplets replaced with the mean values used in the isospin basis, we have obtained again the isospin basis results.

IV. RESULTS

In this Section, we present our result for the scattering length A_{K^-d} . As an introduction, we argue why we think it necessary to go beyond the Fixed Centre Approximation (FCA) as adopted by Kamalov *et al.* [41]. Then we discuss some general aspects regarding the choice of the basis (viz. particle vs. isospin) and the use of different coupled two-body $\bar{K}N$ input, and we investigate the effects due to the choice of different deuteron models. At the end, the effect of "small" two-body input on the K^-d scattering length is discussed.

A. Why need to go beyond FCA ?

In the Introduction, it has been stated that we need to go beyond the FCA and to solve the three-body equation exactly. We justify that claim here.

In the FCA the deuteron is viewed as composed of a proton and a neutron with a fixed separation r . The incoming zero energy K^- -meson then makes multiple scattering off the proton and neutron with no recoil of the target particles. Within this approximation the three-body scattering equation may be solved algebraically: see Eq. (23) of ref. [41], to find the scattering length operator $\hat{A}_{K^-d}(r)$ expressed in terms of the $\bar{K}N$ scattering lengths: a_p , a_n , a_n° , a_{ex} as in Table IV, and the separation r . The actual K^-d scattering length is then identified as the expectation value $\langle \psi_d | \hat{A}_{K^-d} | \psi_d \rangle$ over r with respect to the deuteron wave function $\psi_d(\vec{r})$. So essentially, A_{K^-d} is determined by the two-body $\bar{K}N$ scattering lengths mentioned above. As discussed in Section II, the $\Lambda(1405)$ ($I = 0$) resonance is generated as a bound state of K^-p embedded in the πY continuum. Now the position of this resonance is fairly close to the threshold for K^-p (≈ 1432 MeV) and $\bar{K}^\circ n$ (≈ 1437 MeV), respectively. Thus the elastic K^-p , charge exchange: $K^-p \rightarrow \bar{K}^\circ n$, and hence the elastic $\bar{K}^\circ n$ scattering are all affected by this resonance, and the corresponding amplitudes vary rapidly near their thresholds: see Fig. 4 for the case of the elastic K^-p amplitude which shows strong variations, particularly in its real part. The question then arises as to at which energy these amplitudes should be calculated to produce the corresponding scattering length in use for calculating A_{K^-d} in FCA. The binding energy of the deuteron is ≈ 2.25 MeV. In Fig. 5 we show the values of the two-body scattering lengths which enter the FCA calculation and the resultant A_{K^-d} for different values adopted for the $\bar{K}N$ threshold W . We immediately notice that because of the strong variation of the two-body scattering lengths, the corresponding A_{K^-d} varies also rapidly with a slight shift in W : the real part in particular. This demonstrates that just because of the proximity to the $\Lambda(1405)$ resonance, the FCA is not very reliable. In a full three-body results, the quantity corresponding to W is $\sqrt{\sigma}$: the energy available to any two-body amplitude in the presence of a spectator. This is smeared out due to a loop momentum integration. Consequently, the full three-body results do not suffer from this excessive sensitivity.

B. Calculations including only the $\bar{K}N$ and NN interactions

Here we retain only the deuteron and the $\bar{K}N$ two-body input in the three-body calculation of the K^-d scattering length. This means that in the multiple scattering expansion of the equations only the following three-body states do enter: $K^-(pn)$, $n(K^-p)$, $n(\bar{K}^\circ n)$ and $p(K^-n)$. Although no explicit three-body states with hyperons enter in the calculation in this approximation, there is an implicit effect from the πY channels through the two-body $\bar{K}N$ input. Hence it is more than the *single channel* approximation studied in Ref.[74]. Within the present context we first confront the results from the particle and isospin bases, which makes us keep the result with particle basis in the subsequent subsections. We then study the results with different $\bar{K}N$ models.

1. Isospin and particle bases

The isospin symmetry breaking effects in the $\bar{K}N$ sector have been clearly demonstrated in Sec. II A, by comparing the K^-p observables obtained both in the isospin and particle bases (see Table II, and Figs. 1 and 2). In particular, upon going from the particle to isospin basis, we find that the magnitude of the real part of a_{K^-p} obtained from model "OSA+deuteron-A" decreases by about 20% whereas the imaginary part increases by as much as 30% (see Table II). This last tendency should be due to the fact that in the isospin basis (we reiterate here that in this case the isospin symmetry is exact) two-body channel thresholds become identical among different $\bar{K}N$ channels within the same iso-multiplets. Consequently, these effects are reflected in A_{K^-d} , as one can see Table XI for different $\bar{K}N$ models: by going from the particle to isospin basis, the magnitude of its real part gets smaller by about 10%, while its imaginary part gets strongly enhanced by $\sim 70\%$. In what follows we will mostly comment on the results from the particle basis since they are more realistic.

2. Results using different $\bar{K}N$ models

We give in Table XI the values of A_{K^-d} obtained from models OS1, OSA and OSB of the $\bar{K}N$ interactions described in Section II A. We briefly recall that by construction all the models have adopted the SU(3) symmetry constraint on the strength parameters, with the possible breaking effects introduced in OSA and OSB, and the contributions of the ηY channels have been taken into account, except for OSB. The calculations have been done with model A for

the deuteron. The variation observed on the real and imaginary parts of A_{K-d} calculated in the particle basis are moderate: for example, the real part increases by about 9% and the imaginary part decreases by about 6%, when replacing model OS1 by model OSA. The absolute values of these variations are comparable to those observed in the K^-p scattering length (see Table II): by going from OS1 to OSA we find an increase in the real part by about 13%. For the imaginary part the corresponding increase is less than 1%.

Concerning the contribution from the ηY channels in the $\bar{K}N$ interactions, we observe the same type of effects, both on a_{K-p} and A_{K-d} . Specifically, compared with the values given by model OSA, both the real and imaginary parts of a_{K-p} decrease by $\sim 9\%$ when using OSB (see Table II), while the real part of A_{K-d} increases by $\sim 4\%$ and the imaginary part decreases by $\sim 12\%$. Now we recall the result in Section II A: using model OSA and excluding the contributions of the ηY channels, we have seen that all $\bar{K}N$ observables were strongly affected. In particular, the imaginary part of a_{K-p} increases by as much as $\sim 60\%$, and the real part by $\sim 18\%$ (see Table II). A similar tendency is observed on A_{K-d} , as the OSA value of $(-1.802 + i 1.546)$ fm has been transformed to $(-1.705 + i 2.360)$ fm when the ηY channel contributions are excluded (as discussed in Section II A this means that the coupled channels equations were solved again with the parameters of OSA but excluding the coupling to the ηY channels). In conjunction with the observation in Section II A just mentioned above, we conclude here that it is important to retain these ηY channels for A_{K-d} . Before ending this subsection we should mention that, as shown in our previous publication [1], we have also tested the $\bar{K}N$ amplitude from Ref.[5] in the three-body equation, and the result turned out to be very close to the one with OS1, as expected.

3. Dependence on deuteron models

We have tested three different deuteron models: A, B, C as described in Sec. II B. Their D state probabilities: P_D , are 6.7%, 5.8%, and 0%, respectively. These deuteron models are used in combination with the OS1, OSA and OSB parametrizations of the $\bar{K}N$ interaction, and results are summarized in Table XII. Irrespective of which $\bar{K}N$ model is adopted, there is a definite pattern: the imaginary part of the scattering length increases in accordance with the corresponding increase in the D -state probability of the deuteron. The increase in this quantity due to a change: $P_D = 0 \rightarrow 6.7\%$, is as large as 20%. The real part appears to stay more or less the same in the meantime. We have looked at a few first terms in the three-body multiple scattering series, but that does not tell us why the change is almost exclusively in the imaginary part. But whether it is in real or imaginary part, the following simple observation should suffice in understanding the change of this magnitude. First, we introduce the S and D component of the deuteron wave function in momentum space as $\psi_S(p)$, $\psi_D(p)$, such that

$$P_S = \int_0^\infty \psi_S^2(p) p^2 dp, \quad P_D = \int_0^\infty \psi_D^2(p) p^2 dp, \quad P_S + P_D = 1, \quad (18)$$

where, for example, we may take $P_S \sim 0.93$, $P_D \sim 0.07$ for model A deuteron. We may then re-write

$$\psi_S(p) = \sqrt{P_S} \phi_S(p), \quad \psi_D(p) = \sqrt{P_D} \phi_D(p), \quad (19)$$

such that both ϕ_S and ϕ_D are normalized to unity. Note here that $\sqrt{P_S} \sim 0.97$ and $\sqrt{P_D} \sim 0.26$, respectively. Then we may express the scattering length in the following manner:

$$A_{K-d} = P_S \langle \phi_S | \tilde{A}_{SS} | \phi_S \rangle + 2\sqrt{P_D P_S} \langle \phi_D | \tilde{A}_{DS} | \phi_S \rangle + P_D \langle \phi_D | \tilde{A}_{DD} | \phi_D \rangle, \quad (20)$$

where \tilde{A} are operators in the space of the deuteron wave function, and the closed brackets mean the integration over the initial and final loop (or off-shell) momenta. In the above expression, it is easy to see that due to the second S - D interference term the result with and without the deuteron D state could differ up to a few 10's of a percent, even though P_D is just about $\sim 6\%$. Of course it is likely that the matrix element $\langle \phi_D | \tilde{A}_{DS} | \phi_S \rangle$ may well be smaller than the one for the first term: $\langle \phi_S | \tilde{A}_{SS} | \phi_S \rangle$, due to a slight angular momentum mismatch between the S and D states. However, when we study the behavior of $\psi_S(p)$ and $\psi_D(p)$, it is easy to observe the following trend: the former is very large at $p = 0$ and decreases rather rapidly down to $p \equiv 0.6 \text{ fm}^{-1}$. The latter is zero at $p = 0$ to start with, but its magnitude increases rapidly up to about $p = 0.6 \text{ fm}^{-1}$, then decreases moderately down to about $p = 2.5 \text{ fm}^{-1}$. The result is that the wave function components become of the same order of magnitude from about $p_{equal} = 0.75 \text{ fm}^{-1}$. On the other hand, we find that p_{equal} is in the sub-threshold region for the K^-p amplitude dominated by the $\Lambda(1405)$ resonance, see Fig. 4. This is imbedded in \tilde{A}_{DS} . For this reason it may be fairly likely that $\langle \phi_D | \tilde{A}_{DS} | \phi_S \rangle$ and $\langle \phi_S | \tilde{A}_{SS} | \phi_S \rangle$ are not very different in magnitude, hence a $\sim 20\%$ increase in the imaginary part of A_{K-d} due to the deuteron D state is possible. So it is important to retain that component.

C. Effects of the "small" two-body input

What we term here as small two-body input are (i) the πY channels resulting from the initial $\bar{K}N$ interaction, (ii) πN appearing with a spectator hyperon, and (iii) the YN interactions with a spectator nucleon in the three-body equations. Here we exclude the channels involving the η meson, recall Tables VII. In this manner, in principle, our equations do satisfy three-body unitarity exactly. It was shown in Refs. [14, 15] that these interactions were very important in the threshold break-up reactions: $K^-d \rightarrow \pi NY$ as they control the final state interactions. Here we want to study these effects in the threshold elastic case. For some convenience, calculations in the isospin basis come back in our discussion.

We take models OS1 and OSA for the $\bar{K}N$ interactions, and model A for the deuteron. Then, we add successively the πN - P_{33} and YN interactions described in Sec. II C. The results are given in Table XIII: the third and fourth columns give the values obtained when only the πN - P_{33} or YN input are added to the $\bar{K}N+d$ input, and in the last column both contributions are taken into account. The effect of the additional two-body input is negligible. This can be easily understood by explicitly writing the three-body equations. For example, let us consider Eq. (13) written in the isospin basis, with the following simplified two-body input: $d + \bar{K}N$ (limited to $I = 0$, without the $\eta\Lambda$ channel contribution) + πN - P_{33} . Using the channel labels as defined in Table VII (with y_1, α_1 simplified into y, α , respectively), the explicit form of the coupled three-body equations is:

$$\begin{cases} X_{dd} = Z_{dy}R_{yy}X_{yd} + Z_{dy}R_{y\alpha}X_{\alpha d} \\ X_{yd} = Z_{yd} + Z_{yd}R_dX_{dd} + Z_{yy}R_{yy}X_{yd} + Z_{yy}R_{y\alpha}X_{\alpha d} \\ X_{\alpha d} = Z_{\alpha\Delta}R_{\Delta}X_{\Delta d} \\ X_{\Delta d} = Z_{\Delta\alpha}R_{\alpha y}X_{yd} + Z_{\Delta\alpha}R_{\alpha\alpha}X_{\alpha d} \end{cases} \quad (21)$$

Using the last equation to express $X_{\alpha d}$ in the first three equations, we see that the πN - P_{33} channel contributes in terms of second or higher order, thus its effect on the low energy K^-d observables like A_{K^-d} should be small, although the resulting πN - P_{33} state in the absence of a spectator Y is nearly on the Δ resonance peak in its two-body center of mass energy. This is consistent with a semi-quantitative estimate of the effect by Kamalov *et al.* [41]. Similar arguments hold for the contribution of the YN interactions, and also when the particle basis is used.

Now, we may need to discuss the problem associated with the fact that the signs of the off-diagonal parameters of the $\bar{K}N$ and YN interactions are undetermined. Let us consider for example the OSA model of the $\bar{K}N$ interaction. As explained in Section II A, the signs of the off-diagonal strengths are those of the $SU(3)$ coefficients given in Tables II and III of Ref. [5]. Now, if these signs are changed, the signs of the corresponding off-diagonal two-body propagators are also changed, but the $\bar{K}N$ observables are not (except the signs of the corresponding scattering lengths). For example, changing the signs of $\lambda_{\bar{K}N-\pi\Sigma}$ both for $I = 0$ and $I = 1$, and/or the sign of $\lambda_{\bar{K}N-\pi\Lambda}$ (which contributes only for $I = 1$), does not affect the observables. Similar conclusions hold for the YN interactions when the sign of $\lambda_{\Sigma N-\Lambda N}$ is reversed. Now, the situation is not so simple in the three-body sector. To examine what happens, we consider the following cases in the isospin basis (we choose the isospin basis for the sake of simplicity in handling labels, but the conclusions are the same in the particle basis):

i) Only the $d+\bar{K}N$ interactions (without the ηY channels contributions) are adopted. The corresponding three-body equations have the form (21), with $Z_{\alpha\Delta} = Z_{\Delta\alpha} = 0$. Thus Eqs. (21) reduce to the first two equations with $X_{\alpha d} = 0$. As these equations do not involve the off-diagonal $\bar{K}N$ - πY propagators, the reaction amplitudes do not depend on the sign of the off-diagonal $\bar{K}N$ - πY coupling constants.

ii) Next, we add the πN - P_{33} two-body channel to the one just mentioned above. Going back to Eqs. (21), it is clear that we obtain the same system of equations if we change the signs of both the off-diagonal $\bar{K}N$ - πY propagators and the $X_{\alpha d}$ and $X_{\Delta d}$ amplitudes. Therefore, the K^-d scattering length will not be affected when changing the signs of the off-diagonal $\bar{K}N$ - πY coupling constants.

iii) Now, we add YN interactions to the model with the $d+\bar{K}N$ interactions, and change the sign of the ΣN - ΛN coupling constant. Then, contrary to the previous case, the K^-d scattering length gets changed. This can be understood by noting that, due to isospin conservation, the Λ exchange in the three-body sector is possible only between the $\pi(\Lambda N)_{I=1/2}$ and $N(\pi\Lambda)_{I=1}$ states (Born term $Z_{\beta_2\alpha_3}$, see Table IX). This "dissymmetry" (comparing with the situation for the Σ exchange) implies that we cannot change simultaneously the signs of the ΣN - ΛN propagators and of some of the three-body amplitudes without changing the original system of equations. However, as explained before, the change in A_{K^-d} does not exceed a few percent (see Table XIII), therefore this problem will not be regarded as an important issue worthy of extensive discussion in the present paper. It should be appropriate to stress in this regard that we do not anticipate any significant lack of precision because we have adopted a separable rank one form for the hyperon-nucleon S -wave interactions (which are the part of the "small" input): we have clearly witnessed that these channels have been found to give only a small effect in the calculation of A_{K^-d} . In particular, if we accept that the YN interactions are dictated by $SU(3)$ symmetry, just like our $\bar{K}N$ two-body input, and thus adjust all the

signs of strengths in our separable potentials, for example, to the corresponding S -wave projected Nijmegen meson exchange potentials [63], then the sign ambiguity will also be gone out of our discussion. In fact the related problem was already studied by Dalitz et al., Ref. [15], who found important variations in the Λp mass spectrum in the threshold break up reaction: $K^-d \rightarrow \pi NY$. This will necessitate us to re-examine the break up channels within our present approach. At present, we assess that the effect of the "small" two-body input is actually not important for the calculation of A_{K^-d} .

V. DISCUSSION

In this Section we present the best estimate for the theoretical value for A_{K^-d} in our three-body approach. Then we discuss what kind of uncertainty should be associated with this value which derives from the effects we have left out in the present calculation.

From the result presented in the last Section, we make the following choice for our preferred value: the one from the combination of the two-body input "OSA+deuteron-A", in the particle basis, see Tables XI and XII for the all set of the results. We have not adopted the values from the calculation explicitly incorporating the hyperon channels which are associated with what we called *small two-body input* in Sec. II: as should be clear from Table XIII, the effects are found to be quite small ($< 3\%$). Besides, effects due to the *sign ambiguity* in the off-diagonal YN amplitudes do not exceed 1%. So we take a conservative estimate of the K^-d scattering length to be

$$A_{K^-d} = (-1.80 + i 1.55) \text{ fm}, \quad (22)$$

to which we may assign a possible uncertainty of a few percent.

We then need to assess the effects which may not have been taken into account in an ordinary three-body equations approach like the present one. The first such processes are possible four-body intermediate states: those with two mesons and two baryons. Diagrammatically, they may be divided into partially and totally connected ones. Of partially connected diagrams, those associated with baryon self energies should be dropped from consideration since we assume to have been dealing with the initial $\bar{K}d$ channel. Then the remaining partially connected diagrams are (i) the ones in which there is a spectator meson and two baryons exchanging a meson, and (ii) the ones with a spectator baryon, and a meson and a baryon exchanging a meson. For the first ones they have already been included effectively in the input baryon-baryon (NN or YN) interactions. Likewise, the second ones are effectively included in the coupled $\bar{K}N$ and πN input since they have been fitted to data. So we have only to worry about the completely connected diagrams. Quite fortunately, except practically for a couple of diagrams³, they are reduced to two baryon (YN) interactions: crossed two meson exchanges, and one meson exchanges with meson-baryon-baryon vertex corrections due to virtual meson creation and absorption across the vertex. So those completely connected diagrams are just the pure two-body intermediate YN channels resulting from absorbing \bar{K} (or π).

We thus should consider only the effects of the meson (K^-) absorption in the K^-d elastic scattering at threshold.

In Ref. [77] the p -wave effect in the low energy $\bar{K}N$ interaction has been studied within the context of an effective chiral Lagrangian. In that work, the effect derives from the s -channel pole contributions (the absorption/re-emission of \bar{K} by a nucleon: $\bar{K}N \rightarrow Y \rightarrow \bar{K}N$). So this could be used as a measure for the meson absorption effect under consideration. The authors have stated that the p -wave effect is quite small: total cross sections change very little, whereas the differential cross sections have improved to follow the trend seen in experimental data. From this publication, what we could possibly exploit as the indicators of the K^- absorption effect semi-quantitatively may be the bare mass of Λ , viz. \widetilde{M}_Λ or the ratio R_c , recall Section II for discussion on the available experimental data for the coupled K^-p channels. In this regard, as found in Table II, the other two ratios: γ and R_n are too sensitive to be used for our objective. We have observed that the change in R_c by the K^- absorption effect (viz. the inclusion of the p -wave in the language of Ref.[77]) is at most $\sim 2\%$, whereas the shift from the bare mass to the physical one due to the same effect for the Λ is about 3% (the corresponding values following Eq.(26) in that publication cannot be used since the basis model for the s -wave $\bar{K}N$ interaction has been modified by readjusting the subtraction constants

³ Those may be classified as meson exchange current terms that are found as diagrams (b) and (c) in the work of Weinberg [75] for the case of the pion-deuteron scattering length. This combination has been calculated earlier by Robilotta and Wilkin [76] and found to contribute less than 3% to the total scattering length. Weinberg's calculation did confirm this earlier result. We may conclude that contribution from the corresponding diagrams for A_{K^-d} be far smaller. This is based upon the forthcoming discussion in the main text, on the comparative study of A_{K^-d} and A_{π^-d} related to the meson absorption effect. Note that as explained in Ref. [75], a combination of diagrams (d) and (e) should give no contribution for the scattering length.

in Eq. (26)). Since the kinetic energy available to the YN system after the K^- absorption in the K^-d system at threshold corresponds to $p_Y^{lab} \geq 1$ GeV/c, the effect of the YN interaction is expected to be small (a reasonable guess may be reached from Fig. 3 in the present article and in Ref.[63]). In such a situation what we have just estimated above may well be interpreted as the effect of the K^- absorption. To be on the conservative side we set this to be a possible correction of a few percent.

Not directly applicable but rather useful information regarding the effect of meson absorption comes from the π^-d scattering length: A_{π^-d} . With the exception of some small effects from $\pi^-d \rightarrow \pi^0 nn$ and $\pi^-d \rightarrow \gamma nn$, the scattering length in this process is purely real if no strong pion absorption effect is in effect, viz. no imaginary part in the absence of pion absorption. With this in mind, earlier model calculations indicated that the effect creates contributions both to real and imaginary parts of the scattering length. An earlier three-body model calculations [78] obtained $\mathcal{R}e(A_{\pi^-d}) \equiv -0.035$, and $\mathcal{I}m(A_{\pi^-d})$ to be between 0.0062 and 0.0075, both in units of the inverse pion mass: m_π^{-1} . What should be emphasized here is that the pion absorption contributes to the real part (commonly termed as the dispersive effect) with just about the same magnitude as the imaginary part, but with the negative sign. This characteristic feature was confirmed by a later calculation in multiple scattering in Ref.[79], and the pion absorption contribution was evaluated to be

$$\Delta A_{\pi^-d}^{abs} \equiv (-0.008 + i 0.011) m_\pi^{-1}. \quad (23)$$

A more complete three-body calculation explicitly including the pion absorption in a fully consistent manner [80] obtained

$$A_{\pi^-d} = (-0.047 + i 0.0047) m_\pi^{-1}. \quad (24)$$

The pion absorption may be seen as contributing roughly 10% to the real part.

A couple of recent papers have reported an extraction of A_{π^-d} from the pionic deuterium atomic transitions, Refs. [33, 81, 82], using the Deser-Trueman formula [25] to find (Coulomb interaction included):

$$A_{\pi^-d}^c = (-0.0259 \pm 0.0011) + i (0.0054 \pm 0.0011), \quad (25)$$

from Ref.[33, 81], and

$$A_{\pi^-d}^c = (-0.0261 \pm 0.0005) + i (0.0063 \pm 0.0007), \quad (26)$$

from Ref. [82], both in units of the inverse pion mass as before. Both of these data are consistent with each other, and particularly the imaginary parts are also consistent with the model calculations in Refs. [78, 80]. However, the real parts are about half the magnitude of the model result in Ref. [80]. If we assume that the experimental result be correct and that the result of the model calculation mentioned above be also correct regarding the sign and size of the absorption contribution to the real part, then the real part of the scattering length without the pion absorption effect should be about $-0.020 m_\pi^{-1}$. Then it appears that the data indicate the pion absorption effect to be very close to 30%. And supposing that we translate this to our present K^-d scattering length, the pure three-body result could not be acceptable. But there is a possible way out of this impasse: in Ref.[33, 81], by combining the data from the pionic hydrogen and pionic deuterium, the value of the scattering length π^-n , or more precisely the isoscalar combination:

$$2b_0^c = a_{\pi^-p}^c + a_{\pi^-n}^c, \quad (27)$$

turned out to be consistent with zero. This *near* vanishing of b_0^c should be expected from current algebra calculations [83], and particularly in the soft pion (viz. zero pion mass) limit (however, we should be reminded in this respect that the extraction of this latter quantity is still rather *model dependent*, see Ref. [33, 81] for details, as well as the consequence from the πN partial wave analyses, see for example Ref. [84]). So if one accept this result, the lowest order pion-deuteron scattering length in a static calculation vanishes, and this is the basic origin of the smallness of $\mathcal{R}e(A_{\pi^-d})$. Consequently, one might well come up with that large pion absorption effect.

Now, this is far from true in the case of the K^-d scattering length where (i) because the kaon cannot be regarded as *soft*, and (ii) because of the predominantly exo-energetic nature of the associated coupled channels, even the lowest order scattering length is neither vanishingly small nor purely real to start with, even without K^- absorption. Hence we may safely abide by the estimate of the kaon absorption effect as discussed earlier, and so we set the effect to be less than 10%. Of course a more quantitative study will have to be done.

Our present calculation has not included any electromagnetic interactions, of which the Coulomb interaction plays the dominant role in the actual hadronic quantities measured. So we now come to discuss the effect of the Coulomb interaction as our last subject for this Section. Here just like what we have done above, we will borrow a good part of our argument below from the π^-p and π^-d scattering length problems. In fact, as long as the aspect related to the

electromagnetic interactions is concerned, replacing π^- by K^- should not alter it in an essential manner. So the first important point to be stressed is the following: all the experimental determination of the π^-p elastic (and $\pi^-p \rightarrow \pi^0n$ charge exchange) scattering lengths extracted from the pionic hydrogen atom level shift and width have taken care of various electromagnetic corrections (including the finite electromagnetic size of the pion, vacuum polarisation effect, etc.) to the Deser-Trueman formula only [33, 81, 82]. As found, for example, in Ref.[85], this correction is up to about 2%. But the effect of the point Coulomb interaction, which is the very basis for the use of the Deser-Trueman formula, has not been taken out. Thus to be more precise, the extracted quantities should carry an index ‘‘c’’ to indicate that the Coulomb effect is still there. This we have done explicitly in what we have written above. In the case of the pion-deuteron scattering length, even this type of electromagnetic corrections to the Deser-Trueman formula has not been attempted. To a large extent the reason should be that the calculation is far more complicated than for the π^-p case. But one may well suspect that a straightforward application of the Deser-Trueman formula to this already explicitly extended system would obviously introduce an error far larger than these sophisticated correction to that very formula.

There have been model dependent but rather detailed calculations relating $a_{\pi^-p}^c$ and a_{π^-p} , the latter being due to the purely strong interaction [27, 86]. It was stated that the difference between the two quantities is just a fraction of a percent. As the same method cannot be applied, a very simply estimate was carried out to relate the corresponding quantities for the π^-d scattering length [27]:

$$A_{\pi^-d}^c/A_{\pi^-d} = \int_0^\infty u_{Deu}^2(2r)\phi_0^2(0,r)dr / \int_0^\infty u_{Deu}^2(2r)r^2dr, \quad (28)$$

where $u_{Deu}(r)$ is the S -wave radial deuteron wave function and $\phi_0(0,r)$ is the S -wave zero momentum Coulomb wave function for a unit charge. Clearly, this is just to semi-quantitatively introduce the distortion of the incoming charged pion due to Coulomb interaction. The result is about 4% increase in the magnitude for A_{π^-d} as compared with its Coulomb included counterpart. However, as we see in the experimentally extracted $A_{\pi^-d}^c$ reported above [81, 82], the error bars are just about the size estimated here. So here again, the Coulomb correction seems to appear quite small. Likewise, the same line of reasoning might well apply to the case of the K^-d scattering length. When translated into the model prediction, a possible allowance should be taken into consideration between the purely strong and Coulomb included scattering lengths, although by its very nature the estimate should be regarded qualitative. To this end it should be useful to refer to the work of Barrett and Deloff [34]. They introduced a set of rather simple K^-d optical potentials and calculated the strong interaction shift and width of the $1S$ atomic level for the kaonic deuterium. Also the optical potentials were used to calculate the purely strong (A_{K^-d}), as well as the Coulomb included ($A_{K^-d}^c$) K^-d scattering lengths. The observation they made was that the Deser-Trueman formula might be inaccurate, and that a blind application of that formula and the identification of the extracted quantity as the K^-d scattering length due only to strong interaction might introduce an error as large as 20%. A word of caution should be due regarding this work: the optical potentials constructed there were quite simple, and strong non-locality expected from the dominance of the $\Lambda(1405)$ was absent. So a more realistic optical potential should be constructed in order to give more reliable statements on the issues. Otherwise, if one wants to simply obtain the Coulomb included K^-d scattering length, it is possible to use the pure-strong K^-d amplitude and apply Coulomb corrections as found, for example, in Ref.[87].

VI. SUMMARY AND CONCLUSIONS

The scope of the present work being to develop a reliable formalism to calculate the K^-d scattering length, our starting point was a thorough study of various appropriate two-body processes. For that purpose, we first focused on the highly inelastic K^-p initiated reactions in the kinematics region $p_K^{lab} \leq 250$ MeV/c. The elastic, as well as the relevant seven inelastic coupled-channels were investigated via an effective non-linear chiral meson-baryon Lagrangian. Within a broken SU(3)-symmetry scheme, the adjustable parameters of the formalism were determined by a fitting procedure on the threshold branching ratios and total cross-section data, leading to reduced χ^2 's close to 1.2.

To make clear the sensitivity of the observables to the phenomenological ingredients, three models were constructed. They were then exploited to predict other measured quantities, namely,

- K^-p scattering length, for which our best value is

$$a_{K^-p} = (-0.90 + i 0.87) \text{ fm},$$

in agreement, within the experimental uncertainties, with the recent KEK data,

$$a_{K^-p}^c = (-0.78 \pm 0.15 \pm 0.03) + i(0.49 \pm 0.25 \pm 0.12) \text{ fm}.$$

- The $\Sigma\pi$ mass spectrum, measured at CERN some 20 years ago, was reproduced in an acceptable manner. This quantity was found quite sensitive to the ηY intermediate state within the used coupled-channel approach.

In view of the K^-d system investigations, besides the K^-p interactions, one of course needs another elementary amplitude: K^-n , for which no data is available. We hence performed predictions for the elastic and the four inelastic coupled-channels. Moreover, predictions for various scattering lengths were made, i.e., $a_n(K^-n \rightarrow K^-n)$, $a_n^\circ(\bar{K}^\circ n \rightarrow \bar{K}^\circ n)$, and $a_{ex}(K^-p \rightarrow \bar{K}^\circ n)$. Finally, the implementation of the two-body sector was completed by studying other relevant channels: pion-nucleon, nucleon-nucleon (the deuteron), and nucleon-hyperon interactions.

Then, we moved to the central topic of the present work and developed a relativistic version of the three-body Faddeev equations, to which we embodied the above elementary operators. As expected, this formalism allows us to go far beyond previous investigations, such as single- and multi-channel approaches and fixed center approximation.

As in the case of $\bar{K}N$ interactions, we performed our studies in both isospin and particle bases.

Investigating the K^-d system brings in phenomena with small contributions. A quantitative determination of their importance goes beyond the scope of the present work. However we tried to evaluate them qualitatively, i.e., possible contributions from four-body intermediate states, K^- absorption, and Coulomb correction, this latter being also present in the elementary two-body channels.

Finally, our best value for the K^-d scattering length is,

$$A_{K^-d} = (-1.80 + i 1.55) \text{ fm.}$$

Given the quality of the phenomenological input and approximations introduced, our estimations lead us to attribute to the above values an uncertainty of about 10%.

The awaited for data will soon make clear how realistic our predictions are. These experimental results will come from $D\Phi NE$ on the $\bar{K}N$ and K^-d scattering lengths, as well as from COSY, ELSA, JLab, and SPring-8 on the lowest mass Λ -resonances, including the $\Sigma\pi$ mass spectrum. From theoretical side, several topics deserve to be studied, such as Coulomb effects and K^-d break-up channels.

Acknowledgments

A. B. would like to thank DSM/DAPNIA, CEA/Saclay, and IPN-Lyon for their kind hospitalities. T. M. would like to acknowledge a very pleasant hospitality extended to him at IPN-Lyon where the final phase of the present work was performed. We are grateful to Angels Ramos for informative correspondences on some of her works pertinent to the present one. Thanks go also to Andrej Deloff for discussions on the subject of Coulomb interactions in low energy hadronic systems.

APPENDIX A

Particle and isospin basis

We consider two particles with isospin I_1, I_2 , projections I_{1z}, I_{2z} , and total isospin I, I_z . The transformation from isospin to particle basis is written as:

$$|I_1 I_{1z} I_2 I_{2z}\rangle = \sum_{I=|I_1-I_2|}^{I_1+I_2} \langle I_1 I_{1z} I_2 I_{2z} | II_{1z} + I_{2z}\rangle |II_{1z} + I_{2z}\rangle. \quad (\text{A1})$$

Next, we specify the values of the isospins and their projections of the particles, following the phase convention given in Table I for the isospin states. Calculating the appropriate Clebsch-Gordan coefficients, we easily obtain the linear relations between the states in the two bases.

1. $\bar{K}N$ states

For the K^-p interactions, the eight physical states defined in Eqs. (5) are expressed as linear combinations of the $I = 0, 1$ and 2 states, according to the following relations:

$$\left\{ \begin{array}{l} |K^-p\rangle = \frac{1}{\sqrt{2}} [|00\rangle_{\bar{K}N} - |10\rangle_{\bar{K}N}], \\ |\bar{K}^0n\rangle = \frac{1}{\sqrt{2}} [|00\rangle_{\bar{K}N} + |10\rangle_{\bar{K}N}], \\ |\pi^-\Sigma^+\rangle = -\frac{1}{\sqrt{3}} |00\rangle_{\pi\Sigma} + \frac{1}{\sqrt{2}} |10\rangle_{\pi\Sigma} - \frac{1}{\sqrt{6}} |20\rangle_{\pi\Sigma}, \\ |\pi^+\Sigma^-\rangle = -\frac{1}{\sqrt{3}} |00\rangle_{\pi\Sigma} - \frac{1}{\sqrt{2}} |10\rangle_{\pi\Sigma} - \frac{1}{\sqrt{6}} |20\rangle_{\pi\Sigma}, \\ |\pi^0\Sigma^0\rangle = -\frac{1}{\sqrt{3}} |00\rangle_{\pi\Sigma} + \sqrt{\frac{2}{3}} |20\rangle_{\pi\Sigma}, \\ |\pi^0\Lambda\rangle = |10\rangle_{\pi\Lambda}, \\ |\eta\Sigma^0\rangle = |10\rangle_{\eta\Sigma}, \\ |\eta\Lambda\rangle = |00\rangle_{\eta\Lambda}. \end{array} \right.$$

From these expressions, we can deduce the relations between the transition potentials in the two bases. Choosing a separable form as Eq. (2), with isospin-independent form factors, we obtain the relations between the strength parameters in the two bases. Neglecting the contributions of the $I = 2$ states, we have for example:

$$\lambda_{K^-p-\bar{K}^0n} = \frac{1}{2} [\lambda_{\bar{K}N-\bar{K}N}^0 - \lambda_{\bar{K}N-\bar{K}N}^1] \quad , \quad \lambda_{\bar{K}^0n-\pi^+\Sigma^-} = -\frac{1}{\sqrt{6}} \lambda_{\bar{K}N-\pi\Sigma}^0 + \frac{1}{2} \lambda_{\bar{K}N-\pi\Sigma}^1 \quad , \quad (\text{A2})$$

and so on for the other parameters, with the symmetry property: $\lambda_{ij} = \lambda_{ji}$.

In the case of the K^-n and related states, only the $I = 1$ and 2 states contribute, and the five physical states Eq. (6) are expressed as follows:

$$\left\{ \begin{array}{l} |K^-n\rangle = -|1-1\rangle_{\bar{K}N}, \\ |\pi^-\Sigma^0\rangle = -\frac{1}{\sqrt{2}} |1-1\rangle_{\pi\Sigma} + \frac{1}{\sqrt{2}} |2-1\rangle_{\pi\Sigma}, \\ |\pi^0\Sigma^-\rangle = \frac{1}{\sqrt{2}} |1-1\rangle_{\pi\Sigma} + \frac{1}{\sqrt{2}} |2-1\rangle_{\pi\Sigma}, \\ |\pi^-\Lambda\rangle = |1-1\rangle_{\pi\Lambda}, \\ |\eta\Sigma^-\rangle = |1-1\rangle_{\eta\Sigma}. \end{array} \right.$$

The relations between the strength parameters in the two bases are obtained along the same lines as in the K^-p case. Neglecting as before the $I = 2$ states contributions, we obtain for example:

$$\lambda_{K^-n-K^-n} = \lambda_{\bar{K}N-\bar{K}N}^1 \quad , \quad \lambda_{K^-n-\pi^-\Sigma^0} = \frac{1}{\sqrt{2}} \lambda_{\bar{K}N-\pi\Sigma}^1 \quad (\text{A3})$$

etc.

2. πN states

The different πN states in the particle basis are expressed as linear combinations of the $I = \frac{1}{2}, \frac{3}{2}$ isospin states. Considering the possible charge states of the pion and nucleon, we have the following two sets of coupled states:

$$\left\{ \begin{array}{l} |\pi^0p\rangle = \sqrt{\frac{2}{3}} |\frac{3}{2} \frac{1}{2}\rangle_{\pi N} - \frac{1}{\sqrt{3}} |\frac{1}{2} \frac{1}{2}\rangle_{\pi N}, \\ |\pi^+n\rangle = -\frac{1}{\sqrt{3}} |\frac{3}{2} \frac{1}{2}\rangle_{\pi N} - \sqrt{\frac{2}{3}} |\frac{1}{2} \frac{1}{2}\rangle_{\pi N}, \end{array} \right.$$

$$\left\{ \begin{array}{l} |\pi^-p\rangle = \frac{1}{\sqrt{3}} |\frac{3}{2} -\frac{1}{2}\rangle_{\pi N} - \sqrt{\frac{2}{3}} |\frac{1}{2} -\frac{1}{2}\rangle_{\pi N}, \\ |\pi^0n\rangle = \sqrt{\frac{2}{3}} |\frac{3}{2} -\frac{1}{2}\rangle_{\pi N} + \frac{1}{\sqrt{3}} |\frac{1}{2} -\frac{1}{2}\rangle_{\pi N}, \end{array} \right.$$

and the following single state:

$$|\pi^- n\rangle = \left| \frac{3}{2} - \frac{3}{2} \right\rangle_{\pi N}.$$

Retaining only the contributions with total isospin $3/2$, we deduce from the above expressions the following relations between the strength parameters in the two bases:

$$\lambda_{\pi^0 p - \pi^0 p} = \lambda_{\pi^0 n - \pi^0 n} = \frac{2}{3}\lambda_{\Delta} \quad , \quad \lambda_{\pi^+ n - \pi^+ n} = \lambda_{\pi^- p - \pi^- p} = \frac{1}{3}\lambda_{\Delta}, \quad (\text{A4})$$

etc.

3. ΣN - ΛN states

The ΣN - ΛN states in the particle basis are expressed as linear combinations of the $I = \frac{1}{2}, \frac{3}{2}$ states. We have two sets of three coupled states:

$$\begin{cases} |\Sigma^0 p\rangle = \sqrt{\frac{2}{3}} \left| \frac{3}{2} \frac{1}{2} \right\rangle_{\Sigma N} - \frac{1}{\sqrt{3}} \left| \frac{1}{2} \frac{1}{2} \right\rangle_{\Sigma N}, \\ |\Sigma^+ n\rangle = -\frac{1}{\sqrt{3}} \left| \frac{3}{2} \frac{1}{2} \right\rangle_{\Sigma N} - \sqrt{\frac{2}{3}} \left| \frac{1}{2} \frac{1}{2} \right\rangle_{\Sigma N}, \\ |\Lambda p\rangle = \left| \frac{1}{2} \frac{1}{2} \right\rangle_{\Lambda N}, \end{cases}$$

$$\begin{cases} |\Sigma^- p\rangle = \frac{1}{\sqrt{3}} \left| \frac{3}{2} - \frac{1}{2} \right\rangle_{\Sigma N} - \sqrt{\frac{2}{3}} \left| \frac{1}{2} - \frac{1}{2} \right\rangle_{\Sigma N}, \\ |\Sigma^0 n\rangle = \sqrt{\frac{2}{3}} \left| \frac{3}{2} - \frac{1}{2} \right\rangle_{\Sigma N} + \frac{1}{\sqrt{3}} \left| \frac{1}{2} - \frac{1}{2} \right\rangle_{\Sigma N}, \\ |\Lambda n\rangle = \left| \frac{1}{2} - \frac{1}{2} \right\rangle_{\Lambda N}. \end{cases}$$

and the two following single states:

$$|\Sigma^- n\rangle = \left| \frac{3}{2} - \frac{3}{2} \right\rangle_{\Sigma N},$$

$$|\Sigma^+ p\rangle = \left| \frac{3}{2} \frac{3}{2} \right\rangle_{\Sigma N}.$$

From these relations, we can express the strength parameters in the particle basis in terms of those in the isospin basis. For example, we have:

$$\lambda_{\Sigma^0 p - \Sigma^+ n} = -\lambda_{\Sigma^- p - \Sigma^0 n} = \frac{\sqrt{2}}{3} [\lambda_{\Sigma N - \Sigma N}^{1/2} - \lambda_{\Sigma N - \Sigma N}^{3/2}] \quad , \quad \lambda_{\Sigma^+ n - \Lambda p} = \lambda_{\Sigma^- p - \Lambda n} = -\sqrt{\frac{2}{3}} \lambda_{\Sigma N - \Lambda N}^{1/2}, \quad (\text{A5})$$

and so on.

APPENDIX B

Separable model for coupled channels

The Bethe-Salpeter equation [42] is the relativistic generalization of the Lippmann-Schwinger equation describing the scattering of two particles. In the case of n coupled two-body channels, we have a system of n coupled equations, which reads, in operator form :

$$T_{ij}(\sigma) = V_{ij} + \sum_k V_{ik} G_0^k(\sigma) T_{kj}(\sigma), \quad (\text{B1})$$

with σ the square of the total centre of mass energy. The indices $\{i, j, k\}$ run over the n two-body channels. G_0 is the two-body propagator, V_{ij} the transition potential between channel i and j , and T_{ij} the t -matrix for that transition.

After projecting in the 4-momentum space representation, we obtain a system of 4-dimensional integral equation. Using the Blankenbecler-Sugar (BbS) method (Refs. [43–45]), this equation can be reduced to the following set of coupled three-dimensional equations:

$$T_{ij}(\mathbf{p}_i, \mathbf{p}_j; \sigma) = V_{ij}(\mathbf{p}_i, \mathbf{p}_j; \sigma) + \sum_k \int d^3 p_k V_{ik}(\mathbf{p}_i, \mathbf{p}_k; \sigma) G_0^k(p_k; \sigma) T_{kj}(\mathbf{p}_k, \mathbf{p}_j; \sigma), \quad (\text{B2})$$

where \mathbf{p}_i is the momentum in channel i . The relativistic two-body propagator has the following relativistic expression:

$$G_0^k(p_k; \sigma) = \frac{1}{(2\pi)^3} \frac{\epsilon_1 + \epsilon_2}{2\epsilon_1\epsilon_2[(\epsilon_1 + \epsilon_2)^2 - \sigma]}, \quad (\text{B3})$$

where the two particles in channel k are labeled as 1 and 2, and $\epsilon_i = \sqrt{\mathbf{p}_i^2 + m_i^2}$ is the energy of particle i with mass m_i .

Finally, in the case of s -wave interactions, Eq. (B2) reduces to the following set of coupled one-dimensional integral equations:

$$T_{ij}(p_i, p_j; \sigma) = V_{ij}(p_i, p_j; \sigma) + \sum_k \int_0^\infty p_k^2 dp_k V_{ik}(p_i, p_k; \sigma) G_0^k(p_k; \sigma) T_{kj}(p_k, p_j; \sigma). \quad (\text{B4})$$

Now, we assume that V_{ij} 's are separable, i.e. we write:

$$V_{ij}(p_i, p_j; \sigma) = g_i(p_i) \lambda_{ij}(\sigma) g_j(p_j). \quad (\text{B5})$$

The g 's are the form factors, and $\lambda_{ij}(\sigma)$ is the strength for the transition $i \leftrightarrow j$. Here we assume that in general λ 's are functions of σ . Using this expression in Eq. (B4), we obtain T as separable:

$$T_{ij}(p_i, p_j; \sigma) = g_i(p_i) R_{ij}(\sigma) g_j(p_j), \quad (\text{B6})$$

where R_{ij} is an element of the following $(n \times n)$ matrix:

$$R(\sigma) = [\lambda^{-1}(\sigma) - \tilde{G}(\sigma)]^{-1}. \quad (\text{B7})$$

Here $\lambda(\sigma)$ is an $n \times n$ matrix of the strengths, and $\tilde{G}(s)$ is a diagonal matrix with the following elements:

$$\tilde{G}_{ij}(\sigma) = \delta_{ij} \int_0^\infty p^2 dp g_i^2(p) G_0^i(p; \sigma), \quad (\text{B8})$$

where G_0^i is the relativistic two-body propagator for channel i , calculated from Eq. (B3).

Note that in the case where the strength matrix has no inverse, Eq. (B7) must be re-written as:

$$R(\sigma) = [\mathbf{1} - \lambda(\sigma)\tilde{G}(\sigma)]^{-1}\lambda(\sigma), \quad (\text{B9})$$

where $\mathbf{1}$ is the $(n \times n)$ unit matrix. This situation occurs for example when the $\bar{K}N$ interactions are considered in the particle basis, as the strength parameters obtained as linear combinations of the isospin basis values constitute a matrix with its determinant equal to zero.

APPENDIX C

Antisymmetrization

In the isospin basis, the two nucleons are considered as identical particles. Therefore, one must construct Born terms and three-body amplitudes properly antisymmetrized with respect to the two nucleons. We present hereafter the principle of the method, and we refer the reader to Refs. [17, 45] for more details.

Let us label the two nucleons as N_1 and N_2 . The d channel corresponds to $\widetilde{\overline{K}}(\widetilde{N_1 N_2})$, where the tilde means that the deuteron wave function is properly antisymmetrized. We must also add the nucleons labels to the labels defined in Table VII: $\Delta^i = \Sigma(\pi N_i)$, $\beta^i = \pi(Y N_i)$, $\alpha^i = N_i(\pi Y)$, with $i = 1, 2$, and $y^i = N_j(\overline{K} N_i)$, with $i, j = 1, 2$ ($i \neq j$). (note that the lower indices have been removed, since they do not participate in this discussion).

Now, we have two types of Born term, depending on whether one or two nucleons are involved. In the first category, we have $Z_{\Delta\alpha}$, $Z_{\Delta\beta}$, and $Z_{\alpha\beta}$. For these terms, we only need to introduce the nucleon index. For example, we define: $Z_{\Delta^1\alpha^1} = \langle \Sigma(\pi N_1) | G_0 | N_1(\pi\Sigma) \rangle$, $Z_{\Delta^2\alpha^2} = \langle \Sigma(\pi N_2) | G_0 | N_2(\pi\Sigma) \rangle$, where G_0 is the three-body propagator. Since nucleons 1 and 2 are identical, it is clear that these two Born terms are identical, and we will set: $\tilde{Z}_{\Delta\alpha} = Z_{\Delta^1\alpha^1} = Z_{\Delta^2\alpha^2}$. In the same way, we define: $\tilde{Z}_{\Delta\beta} = Z_{\Delta^1\beta^1} = Z_{\Delta^2\beta^2}$, and: $\tilde{Z}_{\alpha\beta} = Z_{\alpha^1\beta^1} = Z_{\alpha^2\beta^2}$.

The Born terms involving two nucleons, namely Z_{dy} and Z_{yy} , must be antisymmetrized. As the d state is already antisymmetric, we only need to antisymmetrize the y state. So, using the notations defined above, the antisymmetric Z_{dy} Born term will be defined as:

$$\tilde{Z}_{dy} = \langle \widetilde{\overline{K}}(\widetilde{N_1 N_2}) | G_0 \frac{1}{\sqrt{2}} [| N_2(\overline{K} N_1) \rangle - | N_1(\overline{K} N_2) \rangle] = \frac{1}{\sqrt{2}} [Z_{dy^1} - Z_{dy^2}]. \quad (C1)$$

Exchanging N_1 and N_2 in Z_{dy^1} , it is obvious that: $Z_{dy^1} = -Z_{dy^2}$, thus:

$$\tilde{Z}_{dy} = \sqrt{2} Z_{dy^1}. \quad (C2)$$

We proceed along the same lines to define the antisymmetric Z_{yy} Born term:

$$\tilde{Z}_{yy} = \frac{1}{\sqrt{2}} [\langle N_2(\overline{K} N_1) | - \langle N_1(\overline{K} N_2) |] G_0 \frac{1}{\sqrt{2}} [| N_2(\overline{K} N_1) \rangle - | N_1(\overline{K} N_2) \rangle]. \quad (C3)$$

As \overline{K} can be exchanged only between the $(\overline{K} N_1)$ and $(\overline{K} N_2)$ pairs, we have:

$$\tilde{Z}_{yy} = -\frac{1}{2} [\langle N_2(\overline{K} N_1) | G_0 | N_1(\overline{K} N_2) \rangle + \langle N_1(\overline{K} N_2) | G_0 | N_2(\overline{K} N_1) \rangle] = \frac{1}{2} [Z_{y^1 y^2} + Z_{y^2 y^1}]. \quad (C4)$$

Due to the identity of the two nucleons, we have: $Z_{y^1 y^2} = Z_{y^2 y^1}$, and thus:

$$\tilde{Z}_{yy} = -Z_{y^1 y^2}. \quad (C5)$$

For the practical calculation, only the coefficients appearing in the expressions of the antisymmetric Born terms are important, and we can ignore the nucleons labels.

Concerning the two-body propagators, the nucleons labels can be ignored, since only one nucleon is eventually involved in the propagating pair. (the deuteron propagator corresponds to a properly symmetrized 3S_1 or 3S_1 - 3D_1 state).

Finally, the three-body equations can be rewritten in the same form as Eq. (13), where now the Born terms are the antisymmetric terms as defined above.

[1] A. Bahaoui, C. Fayard, T. Mizutani, and B. Saghai, Phys. Rev. C **66**, 057001 (2002).

[2] A.D. Martin, Nucl. Phys. **B179**, 33 (1981); and References therein.

[3] C.B. Dover and G.E. Walker, Phys. Rep. **89**, 1 (1982).

[4] A. Olin and T.-S. Park, Frascati Phys. Series Vol. XVI, 627 (2002); Nucl. Phys. **A691**, 295 (2001).

[5] E. Oset and A. Ramos, Nucl. Phys. **A635**, 99 (1998).

- [6] C.J. Batty, Nucl. Phys. **A508**, 89c (1990).
- [7] J.D. Davies *et al.*, Phys.Lett. **83B**, 55 (1979); M. Izycki *et al.*, Z. Phys. A **297**, 11 (1980); P.M. Bird *et al.*, Nucl. Phys. **A404**, 482 (1983).
- [8] J.H. Hetherington and L.H. Schick, Phys. Rev. **137**, B935 (1965).
- [9] R.H. Dalitz and S.F. Tuan, Ann. Phys. **10**, 307 (1960).
- [10] J.H. Hetherington and L.H. Schick, Phys. Rev. **156**, 1647 (1967).
- [11] J.H. Hetherington and L.H. Schick, Phys. Rev. **141**, 1314 (1966).
- [12] F. Myhrer, Phys. Lett **45B**, 96 (1973).
- [13] L.H. Schick and B.F. Gibson, Z. Phys. A **288**, 307 (1978).
- [14] G. Toker, A. Gal, and J.M. Eisenberg, Nucl. Phys. **A362**, 405 (1981).
- [15] M. Torres, R.H. Dalitz, and A. Deloff, Phys. Lett. **174B**, 213 (1986).
- [16] A. Bahaoui, C. Fayard, G.H. Lamot, and T. Mizutani, Nucl. Phys. **A508**, 335c (1990).
- [17] A. Bahaoui, Thèse de Doctorat, UCBL (1990).
- [18] L.W. Alvarez, UCRL Report No. 9354 (1960).
- [19] T.H. Tan, Phys. Rev. Lett. **23**, 395 (1969); Phys. Rev. **D7**, 600 (1973).
- [20] E.M. Henley, M.A. Alberg, and L. Wilets, Nucleonic **25**, 567 (1980); P. J. Fink, G. He, R.H. Landau, and J.W. Schnick, Phys. Rev. C **41**, 2720 (1990).
- [21] P.B. Siegel and B. Saghai, Phys. Rev. C **52**, 392 (1995).
- [22] T.-S. H. Lee, J.A. Oller, E. Oset, and A. Ramos, Nucl. Phys. **A643**, 402 (1998).
- [23] N. Kaiser, P.B. Siegel, and W. Weise, Nucl. Phys. **A594**, 325 (1995); N. Kaiser, T. Waas and W. Weise, Nucl. Phys. **A612**, 297 (1997).
- [24] M. Iwasaki *et al.*, Phys. Rev. Lett. **78**, 3067 (1997); T.M. Ito *et al.*, Phys. Rev. C **58**, 2366 (1998).
- [25] S. Deser, M.L. Goldhaber, and K. Bauman, Phys. Rev. **96**, 774 (1954); T.L. Trueman, Nucl. Phys. **26**, 67 (1961).
- [26] A. Deloff, AIP Conf. Proc. **603**, 507 (2001).
- [27] A. Deloff, Phys. Rev. C **64**, 065205 (2001).
- [28] S. Bianco *et al.*, Riv. del Nuov. Cim. **22**, No.11, 1 (1999).
- [29] P. Gianotti, nucl-ex/0305010.
- [30] G. Ecker, Prog. Part. Nucl. Phys **35**, 1 (1995).
- [31] C. Guaraldo and B. Lauss, Nucl. Phys. News, Vol. **11** No.2, 20 (2001).
- [32] P. M. Gensini, hep-ph/9804344.
- [33] H.-Ch. Schröder, *et al.*, Eur. Phys. J. C **21**, 473 (2001).
- [34] R.C. Barrett and A. Deloff, Phys. Rev. C **60**, 025201 (1999).
- [35] J.A. Oller, E. Oset, Nucl. Phys. **A620**, 438 (1997); Erratum *ibid*, A **652**, 407 (1999); J.A. Oller, E. Oset, and J.R. Peláez, Phys. Rev. Lett. **80**, 3452 (1998); Phys. Rev. D **59**, 074001 (1999); Erratum *ibid*, **60**, 099906 (1999); J.A. Oller, E. Oset, and A. Ramos, Prog. Part. Nucl. Phys. **45** 157, (2000).
- [36] J.A. Oller and E. Oset, Phys. Rev. D **60**, 074023 (1999).
- [37] J.A. Oller and U. G. Meissner, Nucl. Phys **A673**, 311 (2000); Phys. Lett. **B500**, 263 (2001).
- [38] J. Nieves and E.R. Arriola, Phys. Rev. D **64**, 116008-1 (2001).
- [39] C. Garcia-Recio, J. Nieves, and E.R. Arriola, Phys. Rev. D **67**, 076009 (2003).
- [40] E. Oset, A. Ramos, and C. Bennhold, Phys. Lett. **B527**, 99(2002); Erratum *ibid*, **B530**, 260 (2002).
- [41] S.S. Kamalov, E. Oset, and A. Ramos, Nucl. Phys. **A690**, 494 (2001).
- [42] E.E. Salpeter and H.A. Bethe, Phys. Rev. **84**, 1232 (1951).
- [43] R. Blankenbecler and R. Sugar, Phys. Rev. **142**, 1051 (1966).
- [44] R. Aaron, Modern three hadron physics, editor A.W. Thomas, Springer Verlag (1977).
- [45] N. Giraud, Thèse de spécialité, Université LYON-I (1978).
- [46] G.S. Abraham and B. Sechi-Zorn, Phys. Rev. **139**, 454 (1965).
- [47] M. Csejthey-Barth *et al.*, Phys. Lett. **16**, 89 (1965).
- [48] M. Sakitt *et al.*, Phys. Rev. **139**, 719 (1965).
- [49] W.O.G. Kittel and I. Wacek, Phys. Lett. **21**, 349 (1966).
- [50] J.K. Kim, Columbia Univ. Report, Nevis 149 (1966); Phys. Rev. Lett. **19**, 1074 (1967).
- [51] T.S. Mast *et al.*, Phys. Rev. D **11**, 3078 (1975); *ibid* D **14**, 13 (1976).
- [52] R.O. Bangerter *et al.*, Phys. Rev. D **23**, 1484 (1981).
- [53] J. Ciborowski *et al.*, J. Phys. G **8**, 13 (1982).
- [54] D. Evans *et al.*, J. Phys. G **9**, 885 (1983).
- [55] W.E. Humphrey and R.R. Ross, Phys. Rev. **127**, 1305 (1962).
- [56] D.N. Tovee *et al.*, Nucl. Phys. **B33**, 493 (1971).
- [57] R.J. Nowak *et al.*, Nucl. Phys. **B139**, 61 (1978).
- [58] R.J. Hemingway, Nucl. Phys. **B253**, 742 (1985).
- [59] A. Starostin *et al.*, Phys. Rev. C **64**, 055205 (2001).
- [60] A. Ramos, private communication (2002).
- [61] N. Giraud, C. Fayard, and G.H. Lamot, Phys. Rev. C **21**, 1959 (1980).
- [62] J. Haidenbauer and W. Plessas, Phys. Rev. C **30**, 1822 (1984).
- [63] T.A. Rijken, V.G.J. Stoks, and Y. Yamamoto, Phys. Rev. C **59**, 21 (1999).
- [64] G. Alexander *et al.*, Phys. Rev. **173**, 1452 (1968).

- [65] B. Sechi-Zorn, B. Kehoe, J. Twitty, and R. A. Burnstein, Phys. Rev. **175**, 1735 (1968).
 [66] F. Eisele, H. Filthuth, W. Fölsch, V. Hepp, E. Leitner, and G. Zeth, Phys. Lett. **37B**, 204 (1971).
 [67] R. Engelmann, H. Filthuth, V. Hepp, and E. Kluge, Phys. Lett. **21**, 587 (1966).
 [68] V. Hepp and M. Schleich, Z. Phys. **214**, 71 (1968).
 [69] J.A. Kadyk *et al.*, Nucl. Phys. **B27**, 13 (1971).
 [70] J.M. Hauptman, J.A. Kadyk, and G.H. Trilling, Phys. Rev. **174**, 2022 (1977).
 [71] R. Aaron, R.D. Amado and J.E. Young, Nucl. Phys. **B125**, 29 (1968).
 [72] A.S. Rinat and A.W. Thomas, Nucl. Phys. **A282**, 365 (1977).
 [73] C. Fayard *et al.*, Nuov. Cim. **3A**, 158 (1971); C. Fayard, Thèse de Doctorat d'Etat, Université LYON-I (1975).
 [74] A. Deloff, Phys. Rev. C **61**, 024004 (2000).
 [75] S. Weinberg, Phys. Lett. B **295**, 114 (1992).
 [76] M.R. Robilotta and C. Wilkin, J. Phys G **4**, L115 (1978).
 [77] D. Jido, E. Oset, and A. Ramos, Phys. Rev. C **66**, 055203 (2002).
 [78] I.R. Afnan and A.W. Thomas, Phys. Rev. C **10**, 109 (1974).
 [79] T. Mizutani and D.S. Koltun, Ann. Phys. **109**, 1 (1977).
 [80] C. Fayard, G.H. Lamot, and T. Mizutani, Phys. Rev. Lett. **45**, 524 (1980), and references therein.
 [81] D. Chatellard *et al.*, Phys. Rev. Lett. **74**, 4157 (1995); Nucl. Phys. **A625**, 855 (1997).
 [82] P. Hauser *et al.*, Phys. Rev. C **58**, R1869 (1998).
 [83] S. Weinberg, Phys. Rev. Lett. **17**, 616 (1966); Y. Tomozawa, Nuovo Cim, **46A**, 707 (1966).
 [84] R.A. Arndt, I.I. Strakovsky, and R.L. Workman, Int. J. Mod. Phys. **A18**, 449 (2003).
 [85] D. Sigg *et al.*, Nucl. Phys. **A609**, 316 (1996).
 [86] A. Deloff, Fundamentals in Hadronic Atom Theory, *World Scientific* (2003).
 [87] J. Frölich, B. Saghai, C. Fayard, and G.H. Lamot, Nucl. Phys. A **435**, 738 (1985).

TABLE I: Particle masses (in MeV). The fourth line gives the average mass for each isospin multiplet, and the last line specifies the phase convention used for the isospin states.

K^-	\bar{K}^0	p	n	π^-	π^+	π^0	Σ^-	Σ^+	Σ^0	Λ	η
493.7	497.7	938.3	939.6	139.6	139.6	134.9	1197.4	1189.4	1192.6	1115.7	547.4
\bar{K}		N		π		Σ					
495.7		938.9		138.0		1193.1					
$-\left \frac{1}{2} - \frac{1}{2}\right\rangle$	$\left \frac{1}{2} \frac{1}{2}\right\rangle$	$\left \frac{1}{2} \frac{1}{2}\right\rangle$	$\left \frac{1}{2} - \frac{1}{2}\right\rangle$	$ 1 - 1\rangle$	$- 11\rangle$	$ 10\rangle$	$ 1 - 1\rangle$	$- 11\rangle$	$ 10\rangle$	$ 00\rangle$	$ 10\rangle$

TABLE II: K^-p threshold strong branching ratios and K^-p scattering length (in fm), calculated in the particle basis. The results in the isospin basis are shown in italic letters. See text for experimental data References.

Authors [Ref.]	γ	R_c	R_n	$\mathcal{R}e(a_{K^-p})$	$\mathcal{I}m(a_{K^-p})$	Model
Present work	2.35	0.651	0.189	-0.90	0.87	OSA
	<i>3.17</i>	<i>0.650</i>	<i>0.257</i>	<i>-0.75</i>	<i>1.11</i>	<i>isospin basis</i>
	1.04	0.655	0.130	-0.74	1.41	OSA, ηY excluded
	2.36	0.657	0.193	-0.98	0.80	OSB
Bahaoui et al.[1]	2.38	0.636	0.171	-1.04	0.83	OS1
	<i>3.37</i>	<i>0.626</i>	<i>0.244</i>	<i>-0.95</i>	<i>1.08</i>	<i>isospin basis</i>
Oset & Ramos [5]	2.32	0.627	0.213	-1.00	0.94	Chiral ηY included
	<i>3.29</i>	<i>0.617</i>	<i>0.292</i>	<i>-0.85</i>	<i>1.24</i>	<i>isospin basis</i>
	1.04	0.637	0.158	-0.68	1.64	Chiral ηY excluded
Experiment	2.36 ± 0.04	0.664 ± 0.011	0.189 ± 0.015	$-0.78 \pm 0.15 \pm 0.03$	$0.49 \pm 0.25 \pm 0.12$	

TABLE III: Minimization results for the adjustable SU(3)-symmetry breaking coefficients of models OSA and OSB for the $\bar{K}N$ interactions. For OS1, these coefficients are equal to 1, the average meson decay constant is $f = 1.20f_\pi$, and the range is 870 MeV. We use $f_\pi=93$ MeV/c. The reduced χ^2 are roughly 1.2.

Isospin Channel		OSA	OSB
	f	$1.20 f_\pi$	$1.12 f_\pi$
0	$\bar{K}N$	0.994	1.048
	$\bar{K}N-\pi\Sigma$	1.108	0.917
	$\bar{K}N-\eta\Lambda$	0.851	0.
	$\pi\Sigma$	0.903	0.926
1	$\bar{K}N$	1.056	0.833
	$\bar{K}N-\pi\Sigma$	1.293	1.209
	$\bar{K}N-\pi\Lambda$	0.943	0.933
	$\pi\Sigma$	0.991	1.290
	$\bar{K}N-\eta\Sigma$	0.757	0.
range (MeV)		888.7	879.6

TABLE IV: $\bar{K}N$ scattering lengths (in fm) calculated in the particle basis with models OS1 and OSA. The values in the last column have been evaluated by Ramos [60] at the same energy. a_p , a_n° and a_{ex} (calculated at $W = M_{K^-} + M_p$) are the scattering lengths for elastic K^-p , $\bar{K}^\circ n$, and charge exchange $K^-p \leftrightarrow \bar{K}^\circ n$, respectively. a_n (calculated at $W = M_{K^-} + M_n$) is the scattering length for elastic K^-n .

Reactions	OSA	OS1	Oset-Ramos
$a_p(K^-p \rightarrow K^-p)$	$-0.888 + i 0.867$	$-1.035 + i 0.828$	$-1.013 + i 0.947$
$a_n(K^-n \rightarrow K^-n)$	$0.544 + i 0.644$	$0.573 + i 0.452$	$0.540 + i 0.531$
$a_n^\circ(\bar{K}^\circ n \rightarrow \bar{K}^\circ n)$	$-0.444 + i 0.998$	$-0.602 + i 0.894$	$-0.516 + i 1.053$
$a_{ex}(K^-p \rightarrow \bar{K}^\circ n)$	$-1.215 + i 0.393$	$-1.365 + i 0.484$	$-1.289 + i 0.484$

TABLE V: Strength and range parameters of the YN interactions.

Isospin Channel	Parameters
1/2 ΣN	-3209.69
ΣN - ΛN	-1739.22
ΛN	-1794.16
3/2 ΣN	3072.26
ΣN range (MeV)	452.300
ΛN range (MeV)	356.981

TABLE VI: YN scattering lengths (in fm) calculated at $W = M_{\Sigma^+} + M_n$ for channels ($\Sigma^+n, \Sigma^0p, \Lambda p$), and $W = M_{\Sigma^-} + M_p$ for channels ($\Sigma^-p, \Sigma^0n, \Lambda n$). The single channels values are : $a_{\Sigma^-n} = -0.454$ ($W = M_{\Sigma^-} + M_n$), and $a_{\Sigma^+p} = -0.455$ ($W = M_{\Sigma^+} + M_p$).

channel	Σ^+n	Σ^0p	Λp	channel	Σ^-p	Σ^0n	Λn
Σ^+n	$0.609 + i 3.618$	$0.834 + i 2.837$	$-0.113 - i 1.595$	Σ^-p	$-0.528 + i 2.505$	$-0.192 - i 1.762$	$0.241 - i 0.996$
Σ^0p		$0.145 + i 2.225$	$-0.089 - i 1.251$	Σ^0n		$-0.137 + i 1.277$	$-0.072 + i 0.721$
Λp			1.893	Λn			1.851

TABLE VII: Labels of the three-body channels. The second line specifies the isospin of the two-body sub-system.

channel	$\bar{K}(NN)$	$N(\bar{K}N)$	$N(\pi\Sigma)$	$N(\eta\Lambda)$	$N(\bar{K}N)$	$N(\pi\Sigma)$	$N(\pi\Lambda)$	$N(\eta\Sigma)$	$\Sigma(\pi N)$	$\pi(\Sigma N)$	$\pi(\Lambda N)$	$\pi(\Sigma N)$
isospin	0	0	0	0	1	1	1	1	3/2	1/2	1/2	3/2
label	d	y_1	α_1	μ_1	y_2	α_2	α_3	μ_2	Δ	β_1	β_2	β_3

TABLE VIII: Matrix of propagators in the isospin basis.

channel	d	y_1	α_1	μ_1	y_2	α_2	α_3	μ_2	Δ	β_1	β_2	β_3
$\bar{K}(NN)$	d	R										
$N(\bar{K}N)$	y_1	R	R	R								
$N(\pi\Sigma)$	α_1	R	R	R								
$N(\eta\Lambda)$	μ_1	R	R	R								
$N(\bar{K}N)$	y_2				R	R	R	R				
$N(\pi\Sigma)$	α_2				R	R	R	R				
$N(\pi\Lambda)$	α_3				R	R	R	R				
$N(\eta\Sigma)$	μ_2				R	R	R	R				
$\Sigma(\pi N)$	Δ								R			
$\pi(\Sigma N)$	β_1									R	R	
$\pi(\Lambda N)$	β_2									R	R	
$\pi(\Sigma N)$	β_3											R

TABLE IX: Matrix of Born terms in the isospin basis. For the non-zero Born terms, the exchanged particle is shown in parentheses.

channel	d	y_1	α_1	μ_1	y_2	α_2	α_3	μ_2	Δ	β_1	β_2	β_3
$\bar{K}(NN)$	d	$Z(N)$			$Z(N)$							
$N(\bar{K}N)$	y_1	$Z(N)$	$Z(\bar{K})$		$Z(\bar{K})$							
$N(\pi\Sigma)$	α_1								$Z(\pi)$	$Z(\Sigma)$		$Z(\Sigma)$
$N(\eta\Lambda)$	μ_1											
$N(\bar{K}N)$	y_2	$Z(N)$	$Z(\bar{K})$		$Z(\bar{K})$							
$N(\pi\Sigma)$	α_2								$Z(\pi)$	$Z(\Sigma)$		$Z(\Sigma)$
$N(\pi\Lambda)$	α_3										$Z(\Lambda)$	
$N(\eta\Sigma)$	μ_2											
$\Sigma(\pi N)$	Δ		$Z(\pi)$		$Z(\pi)$					$Z(N)$		$Z(N)$
$\pi(\Sigma N)$	β_1		$Z(\Sigma)$		$Z(\Sigma)$				$Z(N)$			
$\pi(\Lambda N)$	β_2							$Z(\Lambda)$				
$\pi(\Sigma N)$	β_3		$Z(\Sigma)$		$Z(\Sigma)$				$Z(N)$			

TABLE X: Two-body (L, S, J, I) and three-body (l, Σ, \mathcal{J}) quantum numbers in the isospin basis. The two-body partial waves are labeled as : ${}^{2S+1}L_J$ for NN and YN , $L_{2I,2J}$ for πN , and $L_{I,2J}$ for $\bar{K}N$ and πY . The column labeled as l_a (l_b) corresponds to negative (positive) parity states for odd values of \mathcal{J} , and to positive (negative) parity states for even values of \mathcal{J} . Only the values $l \geq 0$ are retained.

channel		L	S	J	I	Σ	l_a	l_b
$\bar{K}(NN)_{3S_1-3D_1}$	d	0,2	1	1	0	1	$\mathcal{J}+1$	\mathcal{J}
							$\mathcal{J}-1$	
$N(\bar{K}N-\pi\Sigma-\eta\Lambda)_{S_{01}}$	$y_{1-\alpha_1-\mu_1}$	0	1/2	1/2	0	0	\mathcal{J}	\mathcal{J}
						1	$\mathcal{J}+1$	\mathcal{J}
							$\mathcal{J}-1$	
$N(\bar{K}N-\pi\Sigma-\pi\Lambda-\eta\Sigma)_{S_{11}}$	$y_{2-\alpha_2-\alpha_3-\mu_2}$	0	1/2	1/2	1	0	\mathcal{J}	\mathcal{J}
						1	$\mathcal{J}+1$	\mathcal{J}
							$\mathcal{J}-1$	
$\Sigma(\pi N)_{P_{33}}$	Δ	1	1/2	3/2	3/2	1	\mathcal{J}	$\mathcal{J}+1$
							$\mathcal{J}-1$	
						2	$\mathcal{J}+2$	$\mathcal{J}+1$
							\mathcal{J}	$\mathcal{J}-1$
							$\mathcal{J}-2$	
$\pi(\Sigma N-\Lambda N)_{3S_1}$	$\beta_{1-\beta_2}$	0	1	1	1/2	1	$\mathcal{J}+1$	\mathcal{J}
							$\mathcal{J}-1$	
$\pi(\Sigma N)_{3S_1}$	β_3	0	1	1	3/2	1	$\mathcal{J}+1$	\mathcal{J}
							$\mathcal{J}-1$	

TABLE XI: Sensitivity of the K^-d scattering length to the model used for the $\bar{K}N$ interaction. The deuteron is model A. The calculations are done in the particle and isospin bases.

Model	OS1	OSA	OSB
particle basis	$-1.985 + i 1.642$	$-1.802 + i 1.546$	$-1.722 + i 1.354$
isospin basis	$-1.759 + i 2.907$	$-1.636 + i 2.618$	$-1.709 + i 2.247$

TABLE XII: Sensitivity of the K^-d scattering length, calculated in the particle basis, to the model used for the deuteron channel. Models A and B have D -state percentage values of 6.7% and 5.8%, respectively, and model C is pure 3S_1 . Models OS1, OSA and OSB of the $\bar{K}N$ interactions are considered.

Model	A	B	C
OS1	$-1.985 + i 1.642$	$-1.966 + i 1.515$	$-1.975 + i 1.313$
OSA	$-1.802 + i 1.546$	$-1.788 + i 1.435$	$-1.780 + i 1.243$
OSB	$-1.722 + i 1.354$	$-1.703 + i 1.263$	$-1.685 + i 1.128$

TABLE XIII: Contributions of the small two-body input to the K^-d scattering length (values in fm). Models OS1 and OSA are used for the $\bar{K}N$ interaction, and model A for the deuteron. The calculations are done in the particle basis.

Model	$d + \bar{K}N$	$+ \Delta$	$+ YN$	$+ \Delta + YN$
OS1	$-1.985 + i 1.642$	$-1.985 + i 1.663$	$-1.975 + i 1.611$	$-1.974 + i 1.634$
OSA	$-1.802 + i 1.546$	$-1.793 + i 1.562$	$-1.805 + i 1.511$	$-1.796 + i 1.529$

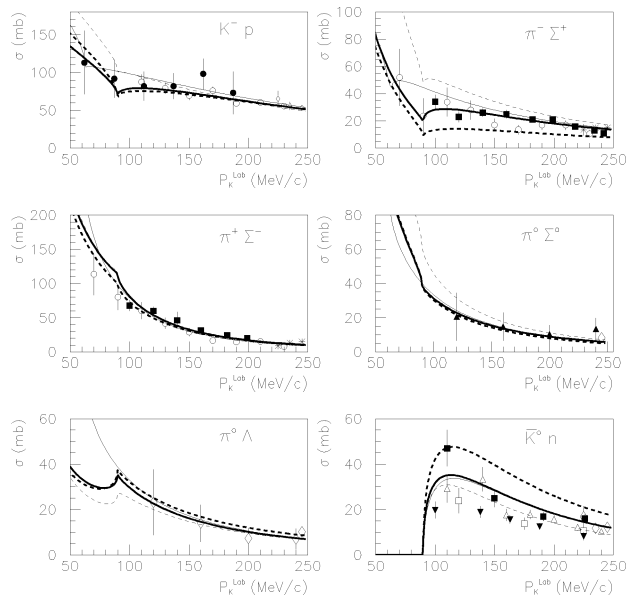


Fig. 1

FIG. 1: Total cross sections initiated by K^-p , calculated in the particle basis with different $\bar{K}N$ models: OSA (bold full line), OS1 (bold dashed line), OSA- η excluded (regular dotted line). The regular full line is obtained with model OSA in the isospin basis. Experimental data are from Refs. [46–54].

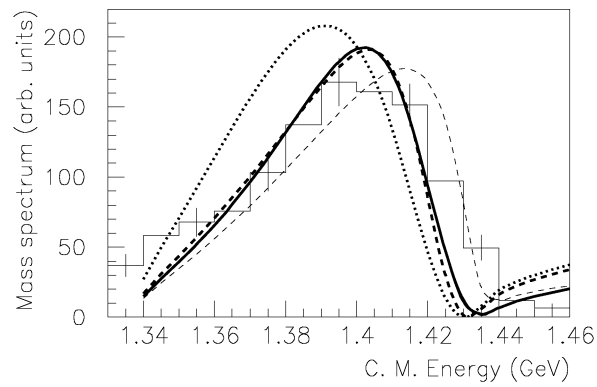


Fig. 2

FIG. 2: $\pi\Sigma$ mass spectrum, obtained with the same models as in Fig. 1. The bold dotted line is model OSB. The OSA results in the isospin and particle bases are practically identical. Experimental data are from Ref. [58].

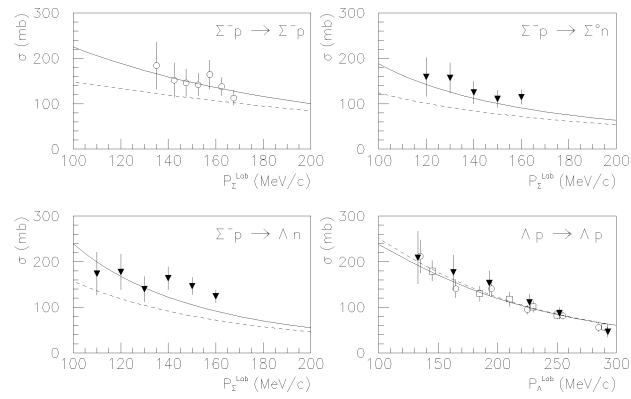


Fig. 3

FIG. 3: $\Sigma^- p \rightarrow \Sigma^- p$, $\Sigma^0 n$, Λn , and $\Lambda p \rightarrow \Lambda p$ total cross sections, calculated in the particle basis (full line) and in the isospin basis (dashed line). Experimental data are from Refs. [64–70].

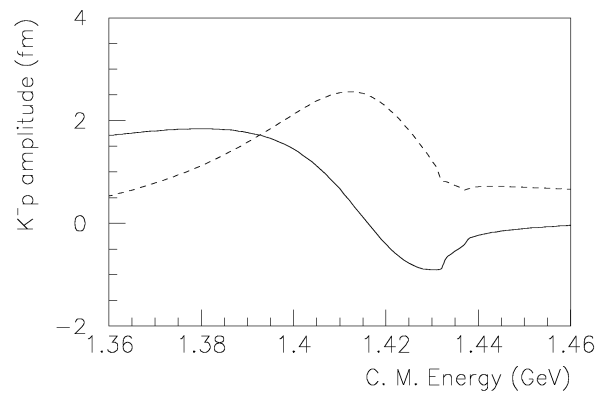


Fig. 4

FIG. 4: K^-p elastic scattering amplitude as a function of the c.m. total energy, calculated in the particle basis with the "OSA+deuteron-A" model. Full line: real part, dashed line: imaginary part.

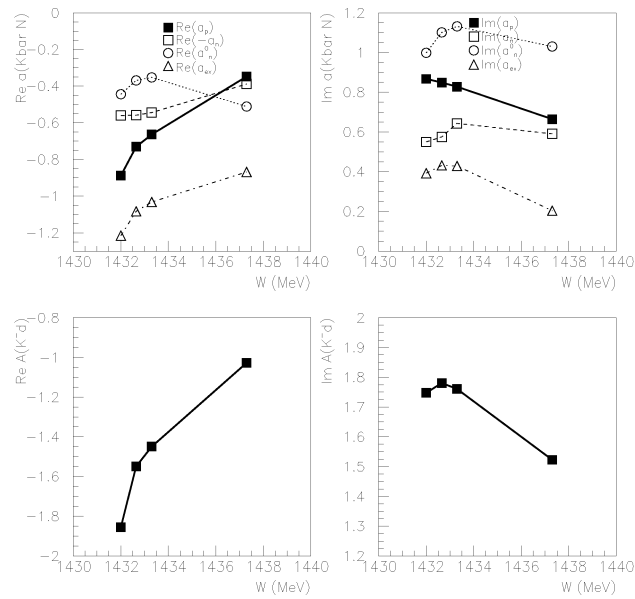


Fig. 5

FIG. 5: $\bar{K}N$ and K^-d scattering lengths calculated in the particle basis for the following values of the two-body threshold energy W : $M_{K^-} + M_p = 1432$ MeV, $M_{K^-} + M_n = 1432.65$ MeV, $M_{K^-} + (M_p + M_n)/2 = 1433.3$ MeV, and $M_{\bar{K}^0} + M_n = 1437.3$ MeV. Model OSA is used for the $\bar{K}N$ interaction. The K^-d scattering length is calculated with the FCA approximation, using the "OSA+deuteron-A" model. Symbols are placed at the threshold values. The lines are to guide the eyes.